iScience

CellPress
OPEN ACCESS

Article

The role of ciliopathy-associated type 3 adenylyl cyclase in infanticidal behavior in virgin adult male mice

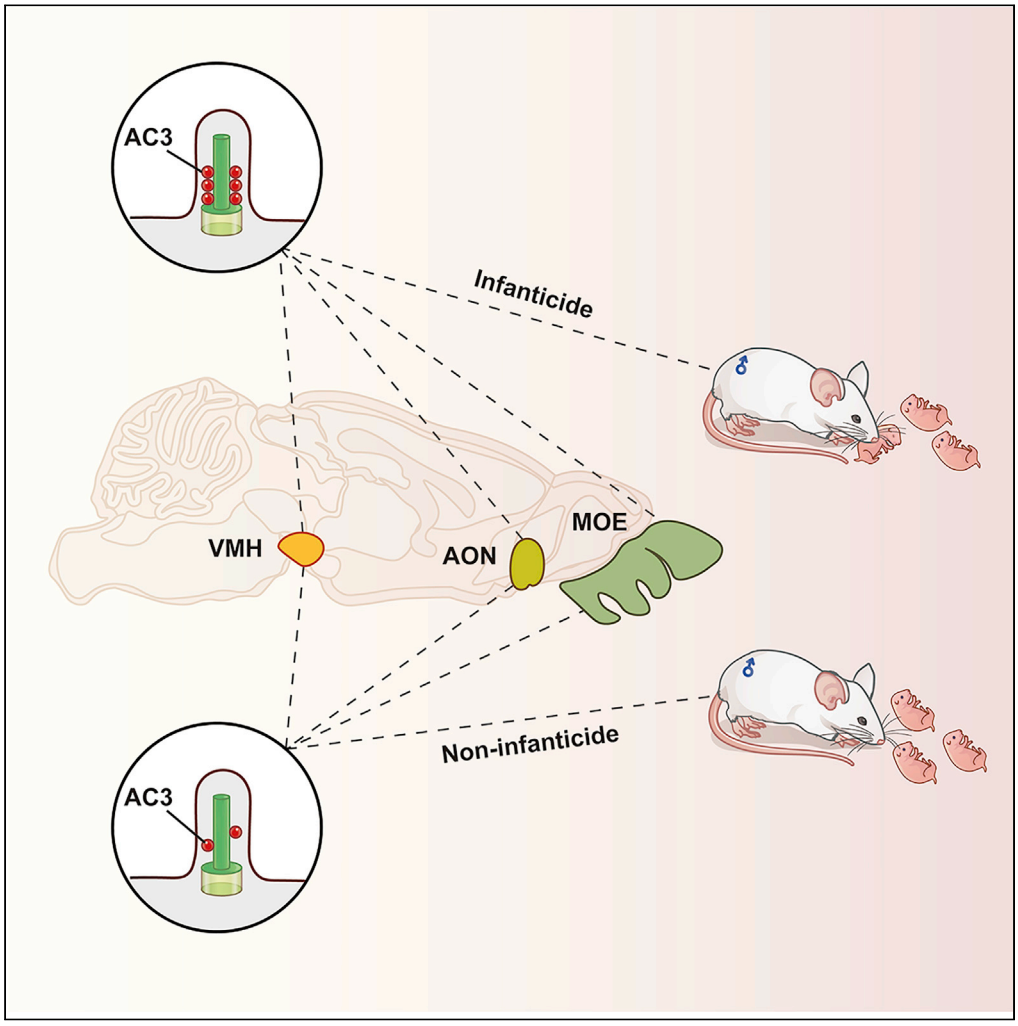

Xiangbo Wu,
Dong Yang,
Yanfen Zhou,
Shujuan Li,
Zhenshan Wang

zswang@hbu.edu.cn

Highlights

MOE lesions and knockdown of AC3 in the MOE result in abnormal infanticidal behavior

The infanticidal behavior of male mice is impaired by lesioning of the AON or VMH

AC3 knockdown in the AON or VMH affects the infanticidal behavior of male mice

Wu et al., iScience 25, 104534
July 15, 2022
https://doi.org/10.1016/j.isci.2022.104534

iScience

CellPress
OPEN ACCESS

Article

The role of ciliopathy-associated type 3 adenylyl cyclase in infanticidal behavior in virgin adult male mice

Xiangbo Wu,[1] Dong Yang,[1] Yanfen Zhou,[1] Shujuan Li,[1] and Zhenshan Wang[1,2,*]

SUMMARY

Virgin adult male mice often display killing of alien newborns, defined as infanticide, and this behavior is dependent on olfactory signaling. Olfactory perception is achieved by the main olfactory system (MOS) or vomeronasal system (VNS). Although it has been established that the VNS is crucial for infanticide in male mice, the role of the MOS in infanticide remains unknown. Herein, by producing lesions via $ZnSO_4$ perfusion and N-methyl-D-aspartic acid stereotactic injection, we demonstrated that the main olfactory epithelium (MOE), anterior olfactory nucleus (AON), or ventromedial hypothalamus (VMH) is crucial for infanticide in adult males. By using CRISPR-Cas9 coupled with adeno-associated viruses to induce specific knockdown of type 3 adenylyl cyclase (AC3) in these tissues, we further demonstrated that AC3, a ciliopathy-associated protein, in the MOE and the expression of related proteins in the AON or VMH are necessary for infanticidal behavior in virgin adult male mice.

INTRODUCTION

Parental behavior is not innate in male animals. As an adaptive reproductive strategy, virgin males often display aggressive behavior toward pups to increase their likelihood of mating (vom Saal and Howard, 1982). This phenomenon of the killing of alien newborn pups by virgin adult males is defined as infanticide (McCarthy and vom Saal, 1985, 1986a, 1986b).

Infanticide is closely related to olfactory signal perception in mice (Isogai et al., 2018; Mennella and Moltz, 1988; Tachikawa et al., 2013; Wu et al., 2014). Mammalian olfactory signal perception is mediated by two anatomically independent organs, namely, the main olfactory epithelium (MOE) and vomeronasal organ (VNO) (Liberles, 2014; Stowers and Kuo, 2015). It is well recognized that infanticidal behavior is highly dependent on VNO system signaling (Isogai et al., 2018; Mennella and Moltz, 1988; Tachikawa et al., 2013; Wu et al., 2014). Surgical VNO ablation or the genetic deletion of VNO signaling components, including Vmn2r65, Vmn2r88, Gαi2, and Trpc2, in adult male mice strongly reduces aggression toward pups (Isogai et al., 2018; Trouillet et al., 2019; Wu et al., 2014). Lesion of the rhomboid nucleus of the bed nuclei of the stria terminalis (BSTrh)—a downstream brain area of the VNO—also impairs infanticidal behavior (Tsuneoka et al., 2015). However, whether main olfactory system (MOS) signaling is needed for the infanticidal behavior of virgin adult male mice has not yet been determined.

The olfactory system is closely connected to the central nervous system (CNS). Olfactory sensory neurons (OSNs) convert chemosensory cues into electronic information and then transmit signals to the brain through the cyclic adenosine-3′-5′-monophosphate (cAMP) signaling pathway (Wong et al., 2000). This signaling pathway is composed of olfactory-specific G protein (Golf), adenylyl cyclase 3 (AC3) and cyclic nucleotide-gated (CNG) channels (Belluscio et al., 1998; Brunet et al., 1996; Wong et al., 2000). The main olfactory bulb (MOB) receives signals from OSNs in the MOE and then transmits the information to the olfactory cortex in the brain (Matsuo et al., 2015; Paxinos, 2004). The anterior olfactory nucleus (AON), as a direct downstream of the MOE, receives chemosensory signals and regulates social behaviors (Matsuo et al., 2015). A lesion of the AON weakens the activity of hypothalamic neurons, which reveals that the hypothalamus can integrate the chemosensory signals received from the MOE-AON (Matsuo et al., 2015).

[1]College of Life Science, Institute of Life Science and Green Development, Hebei University, Baoding 071002, China

[2]Lead contact

*Correspondence: zswang@hbu.edu.cn

https://doi.org/10.1016/j.isci.2022.104534

Global AC3 gene-knockout ($AC3^{-/-}$) mice show impaired olfactory-related behaviors, such as olfactory detection, and aggressive and mating behaviors (Wang et al., 2006; Wong et al., 2000). The detection of pheromones through the AC3 signaling pathway in the MOE plays an important role in olfactory-related behaviors (Wang et al., 2006, 2007). Given that the infanticidal behavior of adult male mice is a newborn pup-evoked pheromone-guided behavior (Tachikawa et al., 2013) and that AC3 is widely expressed in MOS regions (Bishop et al., 2007; Wong et al., 2000), we speculate that the AC3 signaling pathway in the MOS may also be needed for the infanticidal behavior of virgin adult male mice.

In this study, we demonstrated that virgin adult male mice in which the MOE is destroyed through the nasal perfusion of $ZnSO_4$ (5%) show impaired infanticidal behavior. Furthermore, through the combination of CRISPR–Cas9 and nasal perfusion of adeno-associated viruses (AAVs), we generated mice with the specific knockdown (KD) of AC3, a ciliopathy-associated protein or miR-200b/a, which are molecules downstream of AC3, in the MOE, and these males also exhibited deficiency in infanticidal behavior. In addition, through the diffusion of N-methyl-D-aspartic acid (NMDA) and the stereotactic injection of AC3 RNAi AAV, we further found that AC3 expression and either the AON or the ventromedial hypothalamus (VMH) in both areas are indispensable for the infanticidal behavior of virgin adult male mice.

RESULTS

The infanticidal behavior of adult virgin male mice is impaired, whereas their MOE is destroyed

To investigate the role of the MOE in infanticidal behavior, the MOE of adult male mice was ablated through the intranasal injection of 5% $ZnSO_4$ as described in a previous report, and 0.9% NaCl-treated mice were used as controls (Trinh and Storm, 2003; Wang et al., 2006). After 7 days of nasal perfusion, MOE tissues were dissected for histological analysis to assess the degree of destruction. Mature olfactory sensory neurons (mOSNs) are located on the middle and upper layers of MOE tissue. Olfactory marker protein (OMP) is a mOSN marker protein (Farbman and Margolis, 1980). Immunofluorescence (IF) staining showed that almost all mOSNs were eliminated in 5% $ZnSO_4$-treated mice, and these mice only exhibited the basal cell layer in the MOE (Figures 1A and 1B); thus, the thickness of the MOE in the 5% $ZnSO_4$-treated mice was significantly thinner than that of the control mice (Figure 1A). The results indicate that the MOE of the mice was lesioned after the nasal infusion of 5% $ZnSO_4$. Subsequently, we tested the ability of the 5% $ZnSO_4$-treated mice and their controls to distinguish citral and propyl propionate. In the odorant habituation-dishabituation test, the 0.9% NaCl-treated mice could distinguish citral from H_2O and propyl propionate from citral (Figure 1C), but the 5% $ZnSO_4$-treated mice were unable to discriminate the above odorants (Figure 1C). Moreover, the ratio of odorant sniff/water results showed that unlike the NaCl-treated controls, most 5% $ZnSO_4$-treated mice were unable to detect citral and propyl propionate (Figure 1D). The results showed that the olfactory function of the 5% $ZnSO_4$-treated mice was impaired.

The infanticidal behavior of the 5% $ZnSO_4$-treated mice and their controls was observed 7 days after nasal perfusion. Three unfamiliar newborn pups aged 1–2 days were gently introduced into three corners of the cage containing the experimental animals. All the mice rapidly investigated the pups, and no difference in the latency of investigating the pups was found between the 5% $ZnSO_4$-treated mice and their controls (Figure 1E). The control males attacked the pups in 5-min sessions, whereas more than 70% of males with MOE lesions did not show any pup-directed aggressive behavior (Figure 1F), which indicated that the MOE plays an essential role in the infanticidal behavior of adult virgin male mice.

To exclude the impact of VNO damage on infanticidal behavior, we first performed a histological analysis of the VNO of mice. IF staining of OMP and neuron-specific β-III tubulin (Tuj1), a neuronal marker, revealed no significant difference in the number of OMP^+ and $Tuj1^+$ cells in the VNO between the 5% $ZnSO_4$- and 0.9% NaCl-treated mice (Figure S1A), which indicated that the nasal perfusion of 5% $ZnSO_4$ did not affect the structure of the VNO. C-Fos, as an immediate-early response gene, can be used to detect the activation of neurons by sensory input stimuli (Halem et al., 1999). The water-treated negative control mice showed almost no c-Fos expression, whereas the female urine-treated positive control mice showed c-Fos expression in both MOB and AOB regions (Figures S1B–S1D). To further verify the neuronal activity of the VNO, we used 2-heptanone as an odorant stimulus, and performed c-Fos immunocytochemistry to assess the functioning of the VNO in the 5% $ZnSO_4$-treated and control mice. In line with our previous electrophysiology and behavioral studies (Trinh and Storm, 2003; Wang et al., 2006), the results showed that the number of $c\text{-}Fos^+$ cells in the MOB of the 5% $ZnSO_4$-treated mice was significantly lower than that in the control

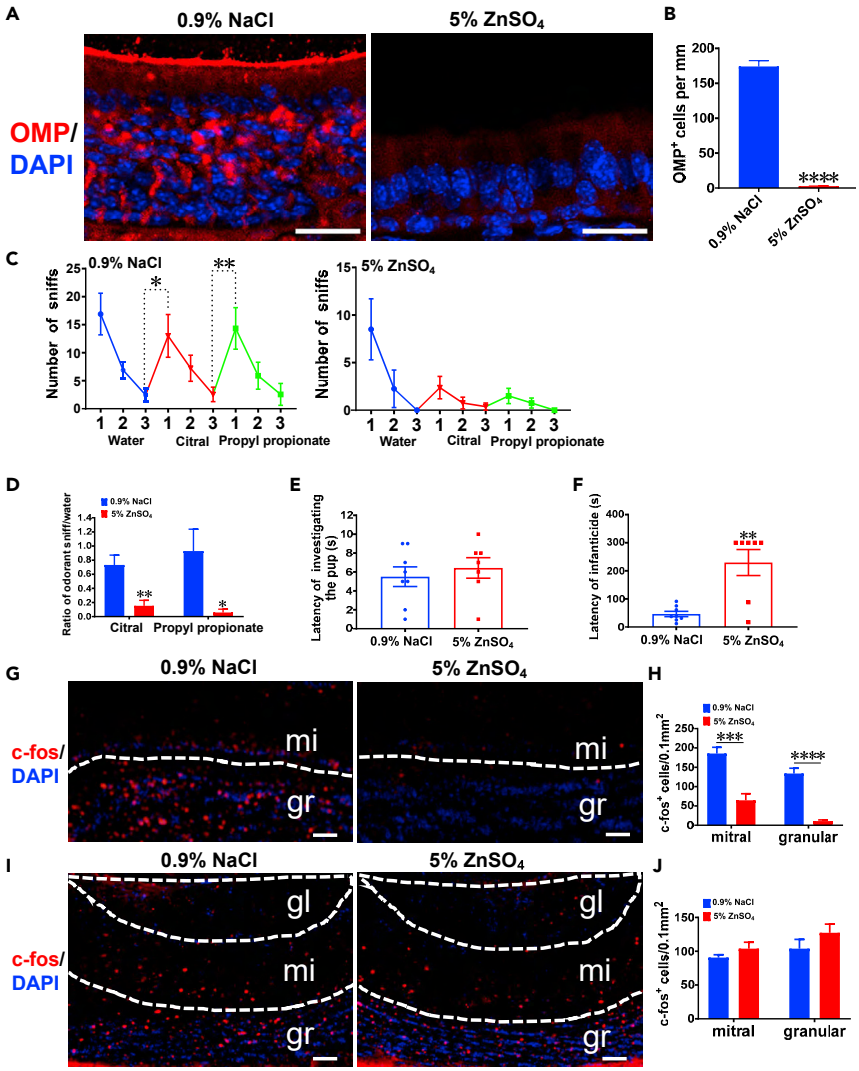

Figure 1. The MOE is critical for infanticidal behavior in adult male mice

(A) IF analysis of OMP in the MOE of 5% $ZnSO_4$-treated mice and their controls. Scale bars, 20 μm.

(B) Quantification of the number of OMP^+ cells in the MOE of 5% $ZnSO_4$-treated mice and their controls (n = 3 mice per group).

(C) The detection of odors, including citral (50 μM) and propyl propionate (50 μM), by the 5% $ZnSO_4$-treated mice and their controls was evaluated through the odorant habituation/dishabituation test. H_2O was used as a negative control (0.9% NaCl-treated mice: n = 9; 5% $ZnSO_4$-treated mice: n = 8).

(D) The ratio of odorant sniffs to water sniffs exhibited by the 5% $ZnSO_4$-treated mice and their controls in the habituation/dishabituation assay. The odorants included citral (50 μM) and propyl propionate (50 μM) (0.9% NaCl-treated mice: n = 9; 5% $ZnSO_4$-treated mice: n = 8).

(E) No significant difference in the latency to investigate the pups was found between the 5% $ZnSO_4$-treated mice and their controls (0.9% NaCl-treated mice: n = 8; 5% $ZnSO_4$-treated mice: n = 7).

(F) Evaluation of the infanticidal behavior showed that the latency to infanticide exhibited by the 5% $ZnSO_4$-treated mice was significantly longer than that in their controls. The duration of the infanticidal behavior test was 300 s (0.9% NaCl-treated mice: n = 8; 5% $ZnSO_4$-treated mice: n = 7).

(G) IF analysis of c-Fos in the mitral and granular cell layers of the MOB of 5% $ZnSO_4$-treated mice and their controls. Scale bars, 100 μm.

(H) Quantification of the number of c-Fos^+ cells in the MOB of 5% $ZnSO_4$-treated mice and their controls (n = 5 mice per group).

(I) IF analysis of c-Fos^+ cells in the mitral and granular cell layers of the AOB of 5% $ZnSO_4$-treated mice and their controls. Scale bars, 100 μm.

(J) Quantification of the number of c-Fos^+ cells in the AOB of 5% $ZnSO_4$-treated mice and their controls (n = 5 mice per group). The data are presented as the mean values ± SEMs; *p < 0.05, **p < 0.01, ***p < 0.001, and ****p < 0.0001, as determined by unpaired two-tailed Student's *t*-test. See also Figure S1.

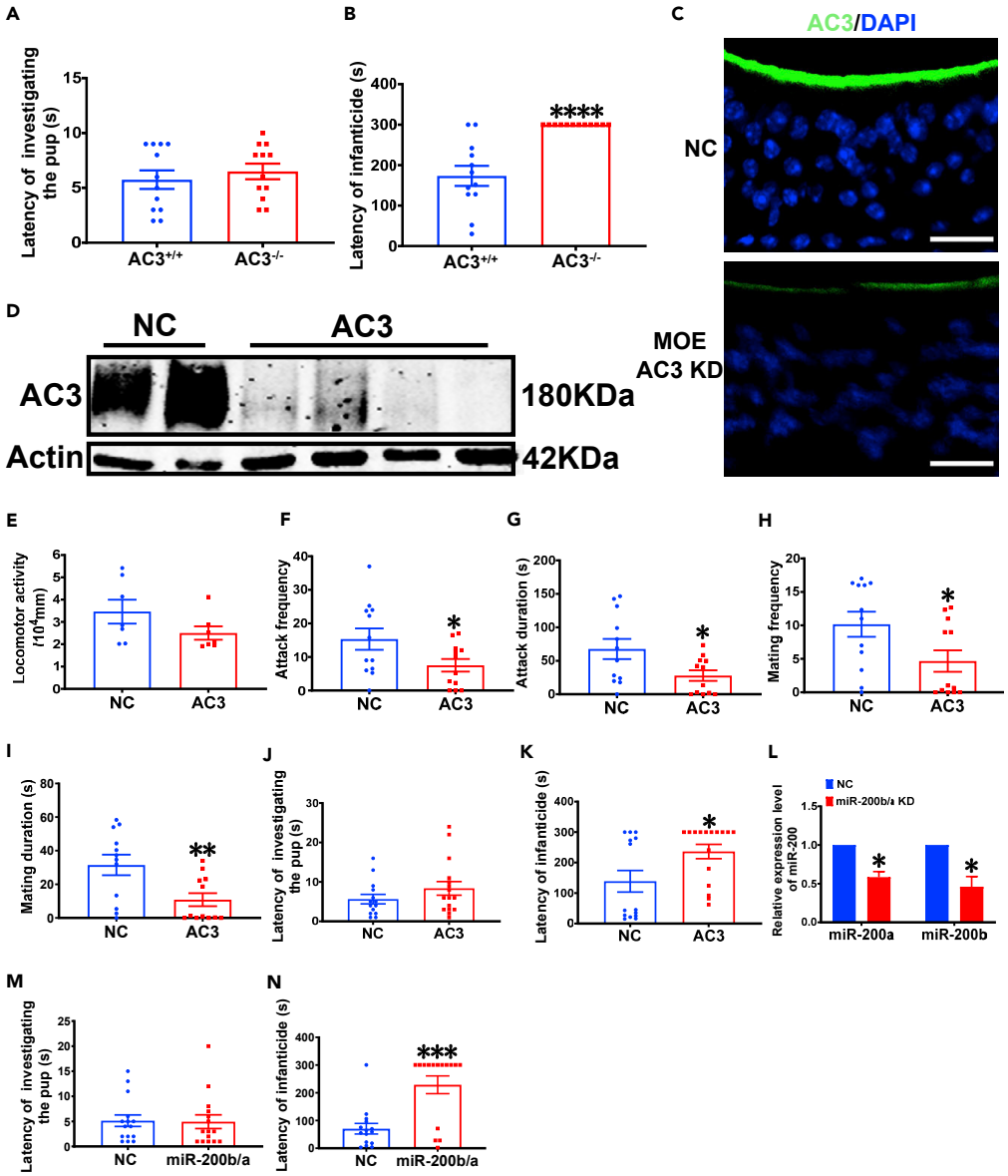

Figure 2. AC3 or miR-200b/a in the MOE is crucial for infanticidal behavior

(A) No significant difference in the latency to investigate the pups was found between the AC3$^{-/-}$ male mice and WT mice (n = 12 per group).

(B) The evaluation of infanticidal behavior showed that the AC3$^{-/-}$ male mice exhibited significantly longer infanticide latencies than the WT mice. The duration of the infanticidal behavior assay was 300 s (n = 12 mice per group).

(C) IF analysis of AC3 in the MOE of MOE-specific AC3-KD mice and NC mice. Scale bars, 20 μm.

(D) WB analysis showing AC3 protein expression in the MOE of MOE-specific AC3-KD mice and NC mice. Actin served as a loading control.

(E) Spontaneous locomotor activity did not differ between the MOE-specific AC3-KD mice and NC mice (n = 7 mice per group).

(F and G) An analysis of aggressive male behaviors showed that the attack frequency (F) and duration (G) of the MOE-specific AC3-KD mice were significantly reduced compared with those of the NC mice (n = 12 mice per group).

(H and I) The male mating behavior test showed that the mating frequency (H) and duration (I) of the MOE-specific AC3-KD mice were significantly reduced compared with those of the NC mice (n = 12 mice per group).

(J) No significant difference in the latency to investigate the pups was found between MOE-specific AC3-KD mice and their controls (NC group: n = 14 mice, AC3-KD group: n = 16 mice).

Figure 2. *Continued*

(K) An evaluation of the infanticidal behavior showed that the infanticide latency of the MOE-specific AC3-KD mice was significantly longer than that of the NC mice. The duration of the infanticidal behavior assay was 300 s (NC group: n = 14 mice, AC3-KD group: n = 16 mice).

(L) A qPCR analysis revealed that the expression of miR-200a and miR-200b in the MOE was significantly decreased in the miR-200b/a-KD mice compared with that of the NC mice (n = 4 mice per group).

(M) No significant difference in the latency to investigate the pups was found between the MOE-specific miR-200b/a-KD mice and their controls (n = 15 mice per group).

(N) An evaluation of infanticidal behavior showed that the infanticidal latency of the miR-200b/a-KD mice was significantly longer than that of the NC mice. The duration of the infanticidal behavior assay was 300 s (n = 15 mice per group). The data are the mean values ± SEMs; *p < 0.05, **p < 0.01, ***p < 0.001, and ****p < 0.0001, as determined by unpaired two-tailed Student's *t*-test. See also Figures S2 and S3.

mice (Figures 1G and 1H), whereas no significant difference was found in the accessory olfactory bulb (AOB) (Figures 1I and 1J), which indicated that the vomeronasal sensory neurons (VSNs) in the 5% $ZnSO_4$-treated mice were still functional. When assessed by the urine preference assay, the 5% $ZnSO_4$-treated mice no longer sniffed the urine of either males or females (Figure S1E), in line with the fact that the behavioral functions of the MOE could not be dissociated from those of the VNO (Matsuo et al., 2015) (see the Discussion section). Nevertheless, we thought that the lack of the infanticidal behavior exhibited by the mice with MOE ablation was not due to abnormalities in the VNO (see the AON section).

AC3 and miR-200b/a in the MOE are vital for the infanticidal behavior of virgin adult males

AC3 is the main signaling component of the MOE (Wong et al., 2000). Thus, the infanticidal behavior of virgin adult male $AC3^{-/-}$ mice was explored. The results showed that all the male mice sniffed the pups first, and no difference in the latency to approach the pups was found between the $AC3^{-/-}$ mice and their controls (Figure 2A). The average latency of infanticide was significantly longer in the $AC3^{-/-}$ mice than in the $AC3^{+/+}$ (wild-type, WT) mice, and almost none of the $AC3^{-/-}$ mice exhibited infanticidal behavior (Figure 2B), which indicated that AC3 gene knockout affects the infanticidal behavior of adult virgin male mice.

AC3 is expressed in the primary cilium of the MOE and brain (Bishop et al., 2007; Wong et al., 2000). Whether these phenotypes exhibited by AC3-knockout mice are caused by anosmia or deficits in the brain is unclear. Therefore, we combined nasal perfusion of AAV with CRISPR/Cas9 gene editing to specifically KD AC3 in adult male mouse MOE tissues. Mice aged 3 months were perfused intranasally with viral vectors (Cas9 AAV combined with AC3 sgRNA or normal control [NC] sgRNA AAV) at a 1:1 ratio. The KD efficiency of the on-target gene achieved with this approach was highest 6–8 weeks after injection (Swiech et al., 2015; Yang et al., 2020). Thus, after 8 weeks of AAV perfusion into the nasal cavity, MOE tissues were dissected for IF and western blot (WB) analysis. Both the IF and WB results illustrated that the expression of AC3 in MOE-specific AC3-KD mice was significantly reduced (Figures 2C and 2D), compared with that in NC mice. To exclude the possibility that the nasal perfusion of AAV affected the expression of AC3 in other tissues, we measured the expression of AC3 in the hypothalamus (downstream region of the MOE signaling pathway). The IF results showed that AC3 expression in the hypothalamus did not differ between MOE-specific AC3-KD mice and NC mice (Figure S2A), which indicated the successful generation of MOE-specific AC3-KD mice.

Although the spontaneous locomotor activity of the MOE-specific AC3-KD mice was indistinguishable from that of the NC animals (Figure 2E), the olfactory-guided male aggressive and male mating behaviors of the MOE-specific AC3-KD mice were impaired (Figures 2F–2I). In the resident/intruder assay, the NC mice continuously attacked the male intruder, whereas the frequency and duration of attack on the intruder males by the MOE-specific AC3-KD mice were significantly reduced (Figures 2F and 2G). Similarly, male mating behavior was analyzed by introducing a WT sexually mature, unfamiliar female into the home cage of each tested male. Although the NC animals showed normal mounting and intromission behaviors toward the female intruder, the frequency and duration of mounting of the females by the MOE-specific AC3-KD mice were distinctly reduced (Figures 2H and 2I). These results show that the KD of AC3 in MOE tissues of mice resulted in defects in olfactory function. The MOE-specific AC3-KD mice aged five months displayed a significantly longer average latency to infanticide than the NC mice, and more than 60% of the MOE-specific AC3-KD mice showed no infanticide but still exhibited a normal pup investigation (Figures 2J and 2K).

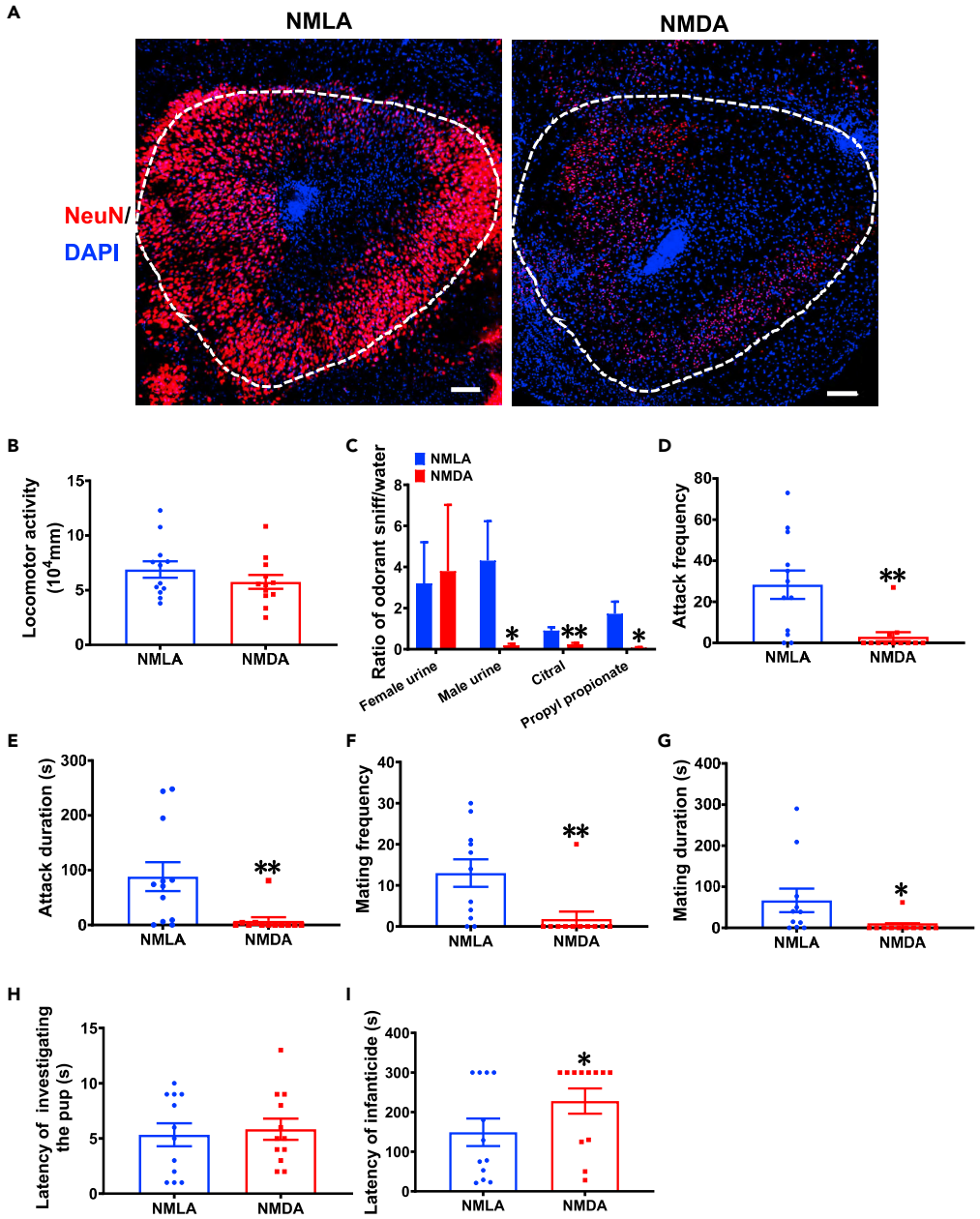

Figure 3. The AON is indispensable for infanticidal behavior

(A) IF analysis of NeuN in the AON of AON-specific NMDA mice and NC mice. Scale bars, 100 μm.

(B) The spontaneous locomotor activity of the AON-specific NMDA mice was similar to that of the NC mice (n = 12 mice per group).

(C) Ratio of odorant sniffs to water sniffs exhibited by the AON-specific NMDA mice and the NC mice in the odorant habituation/dishabituation assay. The odorants included male mouse urine (1:50), female mouse urine (1:50), citral (50 μM), and propyl propionate (50 μM) (male urine, n = 14 mice per group; other odorants, n = 11 mice per group).

(D and E) An analysis of aggressive male behaviors showed that the attack frequency (D) and duration (E) of the AON-specific NMDA mice were significantly reduced compared with those of the NC mice (n = 12 mice per group).

(F and G) The male mating behavior test showed that the mating frequency (F) and duration (G) of the AON-specific NMDA mice were significantly reduced compared with those of the NC mice (n = 11 mice per group).

(H) No significant difference in the latency to investigate the pups was found between the AON-specific NMDA mice and their controls (n = 12 mice per group).

Figure 3. *Continued*

(I) Analysis of infanticidal behavior showed that the infanticide latency of AON-specific NMDA mice was significantly longer than that of the NC mice. The duration of the infanticidal behavior assay was 300 s (n = 12 mice per group). The data are presented as the mean values ± SEMs; *p < 0.05 and **p < 0.01, as determined by unpaired two-tailed Student's *t*-test. See also Figure S4.

To rule out the possibility that the infanticidal behavior of male mice with MOE-specific AC3 KD was caused by VNO dysfunction, we performed IF staining of OMP and Tuj1 in the VNO. The results demonstrated that the number of OMP^+ and $Tuj1^+$ cells in the VNO did not differ between MOE-specific AC3-KD mice and NC mice (Figure S2B). Similar to the findings found for $ZnSO_4$-treated mice, the c-Fos IF results showed that c-Fos^+ cells in the MOB were significantly reduced in the MOE-specific AC3-KD mice compared with NC mice (Figures S3A, S3B and S3D), but no difference in the AOB was found between the MOE-specific AC3-KD mice and NC mice (Figures S3A, S3C and S3D). These results illustrate that MOE-specific AC3-KD mice exhibit normal VSN activity.

MiR-200b/a are downstream molecules of the AC3 signaling pathway in the MOE, and miR-200b/a-KD mice show impaired olfactory behaviors (Yang et al., 2020). Thus, we further explored whether miR-200b/a KD in MOE tissues affects the infanticidal behavior of virgin adult male mice. Viral vectors (Cas9 AAV combined with miR-200b/a sgRNA or NC sgRNA AAV) were perfused intranasally at a 1:1 ratio for the KD of miR-200b/a in the MOE. The expression of both miR-200a and miR-200b was significantly reduced, as determined by qPCR, in the group subjected to 8 weeks of AAV perfusion compared with the control group (Figure 2L), which indicated that miR-200b/a was specifically knocked down in the MOE.

We evaluated the infanticidal behavior of the MOE-specific miR-200b/a-KD mice. The results showed that mice with miR-200b/a KD, particularly in the MOE, showed no difference in latency approaching the pups compared with the control mice (Figure 2M), whereas the latency to infanticide of the MOE-specific miR-200b/a-KD mice was significantly longer than that of the controls, and more than 70% of the MOE-specific miR-200b/a-KD mice showed no infanticidal behavior (Figure 2N). This result indicates that miR-200b/a in the MOE affects the infanticidal behavior of virgin adult male mice.

Taken together, these results demonstrate that the expression of AC3 and miR-200b/a in the MOE is indispensable for the infanticidal behavior of virgin adult male mice.

AON, as a downstream target of the MOE, plays a vital role in the infanticidal behavior of virgin adult male mice

As a direct downstream target of the MOB, the AON might play a vital role in the infanticidal behavior of virgin adult male mice. To explore this hypothesis, N-methyl-D-aspartic acid (NMDA), an excitotoxic amino acid that can eliminate local neurons (Numan et al., 1988; Tsuneoka et al., 2015), was injected into the AON of adult WT male mice (AON-specific NMDA mice), and an equal volume of nontoxic N-methyl-L-aspartic acid (NMLA, an optical isomer of NMDA) was injected into the AON of adult WT male mice as a control (AON-specific NMLA mice). Four days after injection, IF staining of NeuN (a neuron marker protein) was used to detect AON lesions. The results showed that the number of $NeuN^+$ cells in the AON of the AON-targeted NMDA male mice was significantly reduced compared with that in the AON of the control mice (Figure 3A), which indicated that the AON of the adult male mice was destroyed.

Lesion of the AON in adult male mice may affect olfactory-related behaviors. Therefore, AON-specific NMDA and control mice were subjected to odorant detection, male aggressive behavior and male mating behavior tests. The spontaneous locomotor activity of the AON-specific NMDA mice was indistinguishable from that of the control mice (Figure 3B). The odorant habituation/dishabituation test revealed no significant difference in the ability to smell female urine between the AON-specific NMDA mice and the control mice (Figure 3C). However, the ability of the AON-specific NMDA mice to detect citral, male urine and propyl propionate was severely compromised compared with that of the control mice (Figure 3C), which indicated that olfactory detection was partially impaired in mice with AON lesions. Subsequently, we explored the male aggressive and male mating behaviors of the AON-specific NMDA mice and controls. The control mice continuously attacked the intruder, but the frequency and duration of attack on the intruder by the AON-specific NMDA mice were significantly reduced (Figures 3D and 3E). Similarly, the frequency and duration of mounting of the females by the AON-specific NMDA mice were significantly lower than those of the control mice (Figures 3F and 3G). These results showed that olfactory-related behaviors were

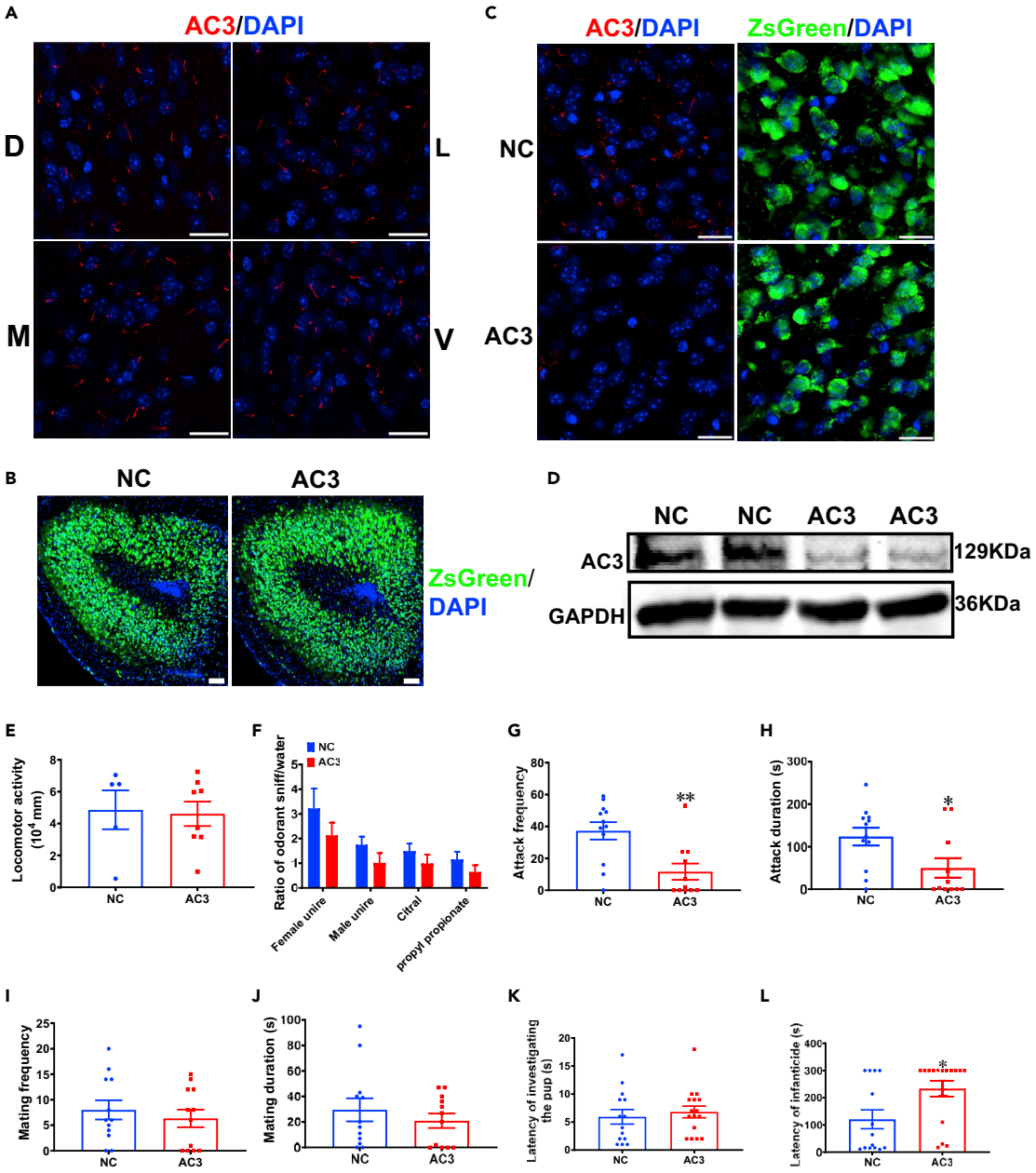

Figure 4. AC3 in the AON is crucial for infanticidal behavior in adult virgin male mice

(A) IF analysis of AC3 in the AON of WT male mice. Scale bars, 20 μm.

(B) AAV infection efficiency in the AON. Scale bars, 100 μm.

(C) IF analysis of AC3 in the AON-specific AC3-KD mice and NC mice. Scale bars, 20 μm.

(D) WB analysis showing AC3 protein expression in the AON of AON-specific AC3-KD mice and NC mice. GAPDH served as a loading control.

(E) The spontaneous locomotor activity of AON-specific AC3-KD mice was similar to that of the NC mice (NC group: n = 5 mice, AC3-KD group: n = 8 mice).

(F) Ratio of odorant sniffs to water sniffs exhibited by the AON-specific AC3-KD mice and NC mice in the odorant habituation/dishabituation assay. The odorants included male mouse urine (1:50), female mouse urine (1:50), citral (50 μM), and propyl propionate (50 μM) (n = 17 mice per group).

(G and H) An analysis of aggressive male behaviors showed that the attack frequency (G) and duration (H) of the AON-specific AC3-KD mice were significantly reduced compared with those of the NC mice (NC group: n = 12 mice, AC3-KD group: n = 11 mice).

(I and J) The male mating behavior test showed that the mating frequency (I) and duration (J) of the AON-specific AC3-KD mice did not differ from those of the NC mice (n = 12 mice per group).

(K) No significant difference in the latency to investigate the pups was found between the AON-specific AC3-KD mice and their controls (NC group: n = 14 mice, AC3-KD group: n = 16 mice).

Figure 4. *Continued*

(L) An analysis of infanticidal behavior showed that the infanticide latency of the AON-specific AC3-KD mice was significantly longer than that of the NC mice. The duration of the infanticidal behavior assay was 300 s (NC group: n = 14 mice, AC3-KD group: n = 16 mice). The data are presented as the mean values ± SEMs; *p < 0.05 and **p < 0.01, as determined by unpaired two-tailed Student's *t*-test. See also Figure S5.

defective in mice with AON lesions. Subsequently, we examined infanticidal behavior and found no difference in the latency to approach the pups between the AON-specific NMDA mice and their controls (Figure 3H). In addition, the latency to infanticide of the AON-specific NMDA mice was significantly longer than that of the controls, and more than 60% of the AON-specific NMDA mice showed no infanticidal behavior (Figure 3I).

To confirm that the noninfanticidal behavior of mice with AON lesions was not caused by MOE impairment, we performed IF staining for AC3 and OMP in the MOE of AON-specific NMDA and control mice. The staining results revealed no difference in either the number of both $AC3^+$ and OMP^+ cells or the thickness of the MOE between the AON-specific NMDA mice and the control mice (Figure S4A), which indicated that the noninfanticidal behavior of the AON-specific NMDA mice was not caused by abnormalities in the MOE. Although the behavioral functions could not be separated in the layer of the MOE from the VNO, the AON received inputs from the MOB but not from the AOB (Matsuo et al., 2015). We speculate that the VNO-dependent behavior might be separated from the MOE by assessing the AON-specific NMDA mice. The urine preference assay results showed that both the AON-specific NMDA mice and their controls preferred the female urine to the male urine (Figure S4B), which indirectly indicated that the noninfanticidal behavior of the AON-specific NMDA mice was not caused by abnormalities in the VNO.

Thus, our results indicated that the AON, as a downstream nucleus of the MOE, also plays a key role in the infanticidal behavior of adult virgin male mice.

Adult virgin male mice show noninfanticidal behavior when AC3 is knocked down in the AON

AC3 is expressed not only in the MOE but also in the AON (Figure 4A). Thus, we hypothesized that AC3 in the AON may play roles in the infanticidal behavior of adult virgin male mice. To investigate this possibility, we administered RNAi-AAV to specifically KD AC3 in the AON of adult WT male mice by injecting an AAV expressing hU6-AC3 shRNA-pCMV-ZsGreen into the AON of 12-week-old mice (AON-specific AC3-KD mice); an hU6-NC shRNA-pCMV-ZsGreen-expressing AAV was used as a control. Four weeks after injection, the infection efficiency of the AAVs in the AON was more than 90% (Figure 4B). IF staining and WB analysis were performed to confirm the efficiency of AC3 KD in the AON. The IF staining results showed that AC3 was expressed on almost all AON neurons in the NCs, whereas the AON-specific AC3-KD mice showed no AC3 expression in more than 80% of AON neurons (Figure 4C). Similarly, the WB analysis revealed that the expression of AC3 in AON-specific AC3-KD mice was significantly reduced compared with that in NC mice (Figure 4D). To rule out the possibility that the stereotaxic surgery performed to inject AAV into the AON affected the expression of AC3 in other regions in the mice, we measured the expression of AC3 in the MOE, OB (upstream of the AON signaling pathway), medial amygdala (MeA) and VMH (downstream of the AON signaling pathway) of AON-specific AC3-KD and control mice. The IF results showed that the levels of AC3 in the MOE, OB, MeA, and VMH did not differ between the AON-specific AC3-KD mice and the controls (Figures S5A–S5D), which indicated that the KD of AC3 in the AON does not influence the expression of AC3 in the other regions. To test whether olfactory-related behaviors were impaired in AON-specific AC3-KD mice, we subjected male AON-specific AC3-KD mice and NC mice to odorant habituation/dishabituation, male aggressive and male mating behavior tests. We first assessed the spontaneous locomotor activity of AON-specific AC3-KD mice and NC mice using the open field test. The results showed that the spontaneous locomotor activity of the AON-specific AC3-KD mice was indistinguishable from that of the NC controls (Figure 4E). The odorant habituation/dishabituation assay was then performed to evaluate whether olfactory detection was impaired in the AON-specific AC3-KD mice. The AON-specific AC3-KD mice exhibited no significant difference in the odorant habituation/dishabituation assay from the NC mice (Figure 4F). Subsequently, we assessed the aggressive behavior of male AON-specific AC3-KD and control mice. Although the NCs consistently attacked the male intruder, the frequency and duration of attack on the intruder males by the AON-specific AC3-KD mice were markedly reduced (Figures 4G and 4H). An evaluation of male mating behavior revealed no significant difference in mating frequency or mating duration between the AON-specific AC3-KD and NC mice (Figures 4I and 4J). These results showed that the KD of AC3 specifically in the AON of adult male mice resulted in partial olfactory-related behavioral defects. Subsequently, the infanticidal behavior of AON-specific AC3-KD mice was tested. The results

suggested that the AON-specific AC3-KD mice still sniffed the pups, and their latency of approaching the pups did not differ from that of the controls (Figure 4K). In addition, the latency to infanticide was significantly prolonged in the AON-specific AC3-KD mice compared with the NC mice, and more than 60% of AON-specific AC3-KD mice showed no infanticidal behavior (Figure 4L). Thus, the results indicated that AC3 in the AON plays a key role in the infanticidal behavior of adult virgin male mice.

The infanticidal behavior of adult virgin male mice is impaired by ablation of the VMH and the KD of AC3 in the VMH

Studies have proven that the hypothalamus can receive and integrate olfactory cues from male urine transmitted through the olfactory organ to trigger aggressive behavior in mice (Chen et al., 2020). We speculated that the VMH may also play a role in the pup-directed aggressive behavior of adult virgin male mice. To further explore this hypothesis, we injected NMDA into the VMH of adult male mice to generate mice with VMH lesions. An equal volume of nontoxic NMLA was injected into adult male mice as a control. Four days after injection, IF staining of NeuN was performed to determine the degree of VMH destruction. The staining results showed that the number of $NeuN^+$ cells in the VMH of the VMH-lesioned mice was significantly lower than that in the control mice, which indicated that the VMH of the adult virgin male mice was lesioned (Figure 5A). Subsequently, infanticidal behavior was examined. The behavior results revealed no difference in the latency for investigating the pups between these mice and their controls (Figure 5B). However, the latency to infanticide of the mice with VMH lesions was significantly longer than that of the mice injected with NMLA into the VMH, and more than 80% of the mice with VMH lesions showed no infanticidal behavior (Figure 5C).

AC3 is highly expressed in the VMH (Bishop et al., 2007). Therefore, we hypothesize that AC3 in the VMH may play an important role in infanticidal behavior. To explore our hypothesis, we knocked down AC3 specifically in the VMH via stereotactic delivery of an AAV expressing U6-AC3 shRNA-pCMV-ZsGreen into the VMH of adult male mice; mice injected with AAV expressing U6-NC shRNA-pCMV-ZsGreen served as controls. We observed an AAV infection efficiency of ~90% in the VMH at 4 weeks after virus injection (Figure 5D). Both IF staining and WB analysis showed that AC3 expression was significantly reduced in the VMH of VMH-specific AC3-KD mice compared with control mice (Figures 5E and 5F). However, in areas surrounding the VMH, the levels of AC3 did not differ between the VMH-specific AC3-KD mice and the control mice (Figures S6A and S6B). We first assessed the spontaneous locomotor activity of VMH-specific AC3-KD mice and NC mice through the open field test. The spontaneous locomotor activity of the VMH-specific AC3-KD mice was indistinguishable from that of the control mice (Figure 5G). Subsequently, infanticidal behavior was examined. The results showed that the latency to infanticide of the VMH-specific AC3-KD mice was significantly longer than that of the controls, and 60% of the VMH-specific AC3-KD mice showed no infanticidal behavior, even though the latency to investigate the pups did not differ between the VMH-specific AC3-KD mice and the control mice (Figures 5H and 5I).

In summary, these results indicate that infanticidal behavior is impaired in adult males with either VMH ablation or AC3 KD in the VMH.

DISCUSSION

Infanticide is a common phenomenon in animals, including insects, fish, amphibians, birds, rodents, felines and primates (Kohl et al., 2017; Lukas and Huchard, 2014). It is well established that pup-derived cues are detected via the vomeronasal system (VNS) (Tachikawa et al., 2013). However, the role of the MOS in infanticidal behavior has not been reported. In this study, we found that the AC3 signaling pathway in the MOE, as well as downstream regions, including the AON and VMH, is crucial for infanticidal behavior in adult virgin male mice.

Intriguingly, one of the characteristic features of infanticidal behavior exhibited by adult virgin male mice is that AC3 disruption in the AON or VMH produces very similar behavioral phenotypes as those obtained by AC3 disruption in the MOE. This finding raises the question of how this finding is possible. The primary cilium is an antenna-like cellular protrusion mediating sensory and neuroendocrine signaling that allows the conversion of external chemical stimuli into intracellular electrical responses in neurons (Menco, 1997). Because AC3 is almost exclusively expressed in the olfactory sensory cilia or primary cilia throughout the central nervous system (CNS) (Bishop et al., 2007; Wong et al., 2000), our results argue that AC3-mediated cAMP signaling in these primary cilia would be crucial for infanticidal behavior.

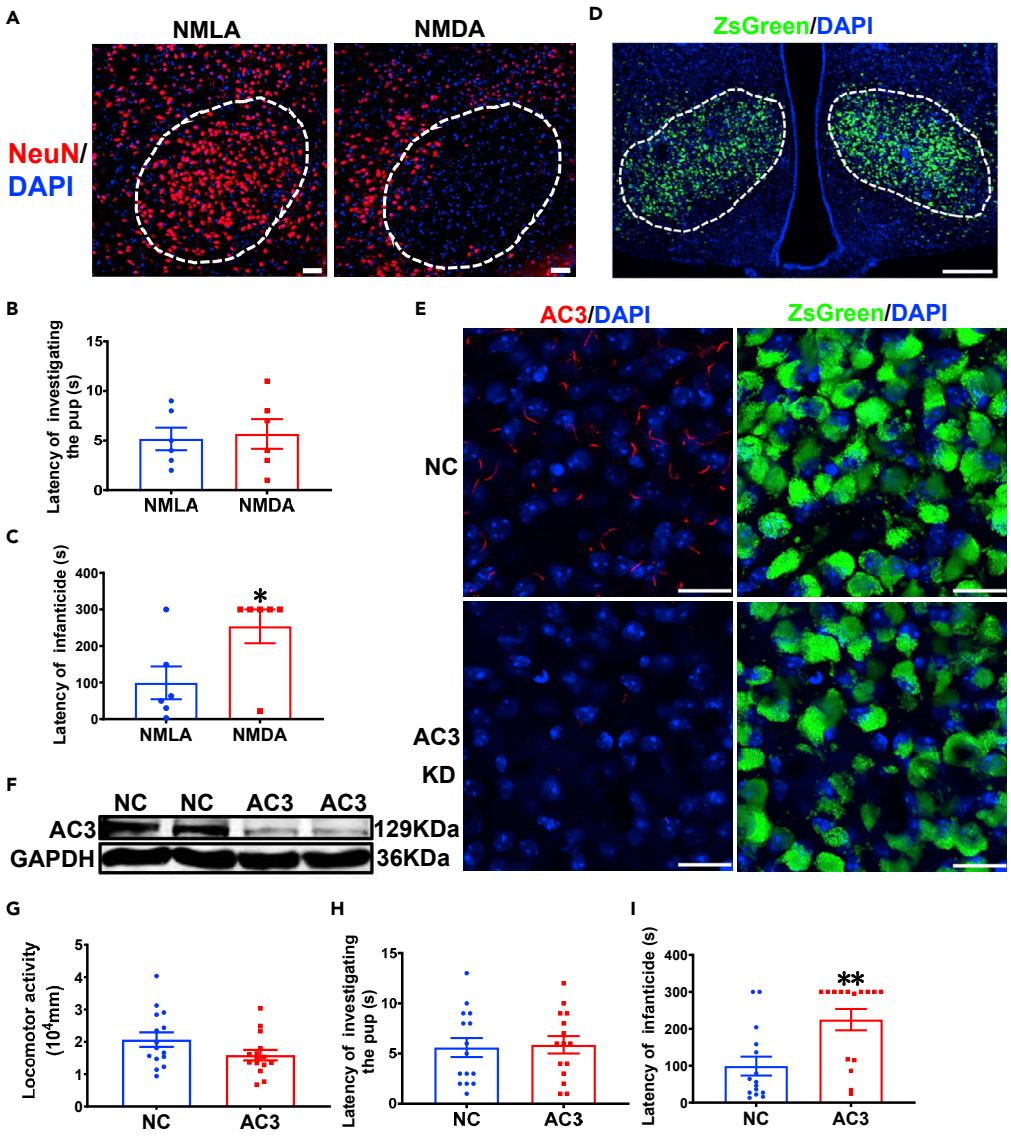

Figure 5. The VMH and AC3 in the VMH are crucial for infanticidal behavior in adult virgin male mice

(A) IF analysis of NeuN in the VMH of VMH-specific NMDA mice and NC mice. Scale bars, 100 μm.

(B) No significant difference in the latency to investigate the pups was found between the VMH-specific NMDA mice and their controls (n = 6 mice per group).

(C) The infanticidal behavior test showed that the infanticide latency of the VMH-specific NMDA mice was significantly longer than that of the NC mice. The duration of the infanticidal behavior assay was 300 s (n = 6 mice per group).

(D) AAV infection efficiency in the VMH. Scale bars, 200 μm.

(E) IF analysis of AC3 in the VMH of VMH-specific AC3-KD mice and NC mice. Scale bars, 20 μm.

(F) WB analysis showing AC3 protein expression in the hypothalamus of VMH-specific AC3-KD mice and NC mice. GAPDH served as a loading control.

(G) The spontaneous locomotor activity of the VMH-specific AC3-KD mice was similar to that of the NC mice (n = 15 mice per group).

(H) No significant difference in the latency to investigate the pups was found between the VMH-specific AC3-KD mice and their controls (n = 15 mice per group).

(I) The infanticidal behavior test showed that the infanticide latency of the VMH-specific AC3-KD mice was significantly longer than that of the NC mice. The duration of the infanticidal behavior assay was 300 s (n = 15 mice per group). The data are presented as the mean values ± SEMs; *$p < 0.05$ and **$p < 0.01$, as determined by unpaired two-tailed Student's *t*-test. See also Figure S6.

In the MOE, the deletion of AC3 causes stronger disorganization in the convergence of the olfactory fibers to the correct OB glomeruli (Col et al., 2007; Trinh and Storm, 2003). Similarly, a functional cilium in the CNS is crucial for maintaining the connectivity of neurons (Bowie and Goetz, 2020; Guo et al., 2017; Haq et al., 2019; Kumamoto et al., 2012; Tereshko et al., 2021), which is highly dependent on ciliary AC3 signaling to tightly regulate the maintenance of the dendritic spine shape, size, and number in a dynamic manner (Chen et al., 2016). Because neuronal circuitry integrity, as well as neuron maturation, sculpted by the dendritic spine and signaling of primary cilium via ciliary AC3 signaling in both the MOE and CNS (Green et al., 2018; Guadiana et al., 2013; Guemez-Gamboa et al., 2014; Guo et al., 2019; Hildebrandt et al., 2011; Lee et al., 2020; Parisi, 2019; Reiter and Leroux, 2017; Sarkisian and Guadiana, 2015; Sun et al., 2021), is strongly associated with neurological and neurodevelopmental linked behaviors, including infanticidal behavior (Amano et al., 2017; Autry et al., 2021; Gipson and Olive, 2017; Kohl, 2020; Kulkarni and Firestein, 2012; Mori and Sakano, 2021), it would appear reasonable to include them in a unitary model in which specialized ciliary AC3 signaling in the MOE, AON, or VMH is needed for maintenance of the infanticidal behaviors in adult virgin male mice, although the interpretation of the exact mechanism remains to be confirmed.

The infanticidal behavior of adult male mice is evoked by the combined effects of hormones, neuropeptides, and neurobiological regulation. It has been revealed that hormonal changes, including testosterone, are linked to the transition from infanticidal to paternal behavior in virgin males (Fukui et al., 2022; Martinez et al., 2015; Romero-Morales et al., 2021; Stagkourakis et al., 2020; Yoshihara et al., 2021). However, our previous data showed that the serum testosterone level is not abnormal in $AC3^{-/-}$ mice (Wang et al., 2006).

Alternatively, oxytocin (OXT) can significantly increase the spontaneous inhibitory postsynaptic current (sIPSC) frequency in medial preoptic area (MPOA)-projection amygdalohippocampal area (AHi) neurons and thereby regulates the infanticidal behavior of male mice (Sato et al., 2020). Furthermore, the onset of puberty in mammals is regulated by hypothalamic gonadotropin-releasing hormone (GnRH) neurons (Messina et al., 2016), which are strongly associated with infanticidal behavior. There is a direct synaptic connection between GnRH neurons and the hypothalamic regions that receive chemical signals from both the VNO and the MOE (Boehm et al., 2005; Yoon et al., 2005). Studies have shown that the cAMP signaling pathway is involved in the secretion of GnRH in immortalized GnRH neurons (GT1–7 cells) (Frattarelli et al., 2011). Circulating hormones, neuropeptides and neurotransmitters might converge on cilia to dynamically adjust intrinsic or synaptic properties and thus modulate infanticidal behaviors in adult virgin males (Fukui et al., 2022; Li et al., 2012; Loktev and Jackson, 2013). Given that AC3 is widely expressed in the primary cilia of the OSN and CNS and that the neuronal cells of $AC3^{-/-}$ mice are blunted in response to neurochemical changes (Wang et al., 2006, 2009), the possibility that the defects in infanticidal behaviors disclosed in this study might be evoked by hormonal signaling occurring in these primary cilia within the CNS that regulates infanticidal behaviors cannot be ruled out, but the details need to be further explored.

The VNO and its signaling component Trpc2 are needed for the infanticidal behavior of adult virgin male mice (Mennella and Moltz, 1988; Tachikawa et al., 2013; Trouillet et al., 2019; Wu et al., 2014). Studies have shown that Trpc2 is also expressed in the MOE (Bleymehl et al., 2016; Omura and Mombaerts, 2015), which indicates that Trpc2 in the MOE may also contribute to defects in infanticidal behavior. However, a recent study showed that Trpc2-mediated signaling in the MOE is independent of Cnga2 and does not depend on intact cilia (Koike et al., 2021), which indicates that Trpc2-mediated signaling in the MOE is unlikely to contribute to the infanticidal behavior of adult virgin male mice.

In contrast, some evidence shows that the MOB and AOB are anatomically and electrophysiologically connected (Vargas-Barroso et al., 2015). The MeA, a crucial area for infanticidal behavior modulations, is a major site for the integration and processing of the environmental sensory information received, and this site then relays the informative neuronal output to the VMH to be analyzed to trigger the associated behavioral response. Although considerable evidence shows that the AOB predominantly sends axons to the MeA, which in turn projects to downstream areas such as the BNST, the medial preoptic area (MPOA), and the VMH, areas involved in controlling infanticidal behaviors (Bergan et al., 2014; Chen et al., 2019; Choi et al., 2005; Dimen et al., 2021; Isogai et al., 2018; Kohl, 2020; Raam and Hong, 2021; Tachikawa et al., 2013; Trouillet et al., 2019; Wu et al., 2014), it is becoming increasingly clear that the MeA also directly or indirectly receives some MOB inputs (Dhungel et al., 2011; Inokuchi et al., 2017; Kang et al., 2009, 2011; Keshavarzi et al., 2015; Matsuo et al., 2015; Mucignat-Caretta, 2021; Perez-Gomez et al., 2015; Pro-Sistiaga et al., 2007; Shao et al., 2021; Thompson et al., 2012).

Furthermore, bidirectional communications among the MOS, VNS, MeA, and VMH have been established in multiple manners (Aqrabawi et al., 2016; Boehm et al., 2005; Inbar et al., 2022; Ishii et al., 2017; Lo et al., 2019) because such signals received by the MOS and VNS interact and converge to work in concert with the integrative circuits of the brain. At another layer, VNS activation needs physical contacts with the stimuli by the so-called vomeronasal pump (Ben-Shaul et al., 2010; Martinez-Garcia et al., 2009; Matsuo et al., 2015; Meredith et al., 1980; Meredith and O'Connell, 1979). Thus, the loss of MOS function may also indirectly influence VNS function by behaviorally isolating animals from chemosensory cues.

Nevertheless, despite the fact that olfactory-guided social behaviors, including infanticide, depend on functional signaling in both the MOS and VNS (Baum and Cherry, 2015; Korzan et al., 2013; Lemons et al., 2017; Pandolfi et al., 2018; Slotnick et al., 2010), functional separation of the MOE from the VNO cannot be achieved at the behavioral level (Matsuo et al., 2015). The ability of adult virgin male mice to detect/discriminate between male and estrous female urinary odors is MOS dependent, as revealed by the odorant habituation/dishabituation assay (Jakupovic et al., 2008; Martel and Baum, 2009; Pankevich et al., 2006; Woodley et al., 2004). In contrast, functional VNS signaling is more likely to be required for the preference of adult male mice for estrous female urinary odors, as exhibited by the urine preference assay (Bayless et al., 2019; Beny-Shefer et al., 2017; Chen et al., 2020; Martel and Baum, 2009; Pankevich et al., 2004, 2006; Woodley et al., 2004), although a functional MOS is also necessary to cooperate with VNS in the execution of this social behavior. Consistent with this fact, our data (Figure S1E) and those of others (Matsuo et al., 2015) showed that the sniffing duration for male and estrous female urinary odors was drastically diminished in mice with defects of MOS signaling. The MOE and VNO can be distinguished by electrophysiology and cellular studies (Trinh and Storm, 2003; Wang et al., 2006). Besides, AC3 is widely expressed in the MOS but not in the VNS (Bishop et al., 2007; Wong et al., 2000). Furthermore, the AON receives inputs from the MOB but not the AOB (Matsuo et al., 2015), and our results shows that the infanticidal behavior is impaired in both the AON-lesioned mice (Figure 3I) and the AON-specific AC3-KD mice (Figure 4L). Thus, our findings indicate that the defects in the infanticidal behavior exhibited by the mice in this study were because of abnormalities in the MOS, although more solid evidence needs to be provided in the future.

The primary cilium, as a signaling hub, may sense dynamic extracellular cues from enriched environments and transduce them into neurons to regulate diverse aspects associated with neuronal development and function. Consequently, the disruption of cilia genesis or cilia-based signaling causes a set of overlapping human disorders, including sensory defects, obesity, infertility, cystic kidney disease, developmental abnormalities, intellectual disability, and mental disorders, which are collectively termed ciliopathies (Anvarian et al., 2019; Reiter and Leroux, 2017). Because AC3 is almost exclusively concentrated in the cilia of diverse neuron types in the brain (Bishop et al., 2007; Sipos et al., 2018), our current results coupled with those from previous studies demonstrate that the ablation of AC3 in mice also leads to pleiotropic phenotypes, including anosmia, cognitive deficit, obesity, and depression-like behaviors, in a brain region-specific and cell type-specific manner (Challis et al., 2015; Chen et al., 2016; Chesler et al., 2007; Col et al., 2007; Guadiana et al., 2013; Liu et al., 2020a, 2020b; Livera et al., 2005; Siljee et al., 2018; Wang et al., 2006, 2009, 2011; Wang and Storm, 2011; Yang et al., 2021, 2022; Zhang et al., 2017; Zhou et al., 2021; Zou et al., 2007). Intriguingly, a recent study showed that neuropilin 2 (Nrp2), an axon guidance molecule, plays crucial roles in instructing circuit formation from the MOB to MeA for the transmission of attractive social signals in the brain (Inokuchi et al., 2017). Given that the role of both neuropilin 1 (Nrp1) and its ligand Sema-3A in axon guidance processes toward the MOB depends on functional ciliary AC3-mediated cAMP signaling in the MOE (Col et al., 2007; Henion et al., 2011; Imai et al., 2009; Schwarting and Henion, 2011) and is associated with cilium-related Hedgehog signaling (Cai et al., 2021; Hillman et al., 2011; Pinskey et al., 2017) and that the ablation of neuropilin and its ligand in mice leads to pleiotropic phenotypes (Assous et al., 2019; Cariboni et al., 2007; Demyanenko et al., 2014; Duncan et al., 2021; Li et al., 2019; Maden et al., 2012; Mohan et al., 2018, 2019; Riccomagno et al., 2012; Tan et al., 2019; Tran et al., 2009; van der Klaauw et al., 2019; Vanacker et al., 2020) that mirror the functions of AC3 in multiple brain areas, we hypothesize that the pleiotropic phenotypes illustrated in these AC3-deficient mice, including the defects in infanticidal behaviors observed in this study, might be caused by cilia-associated neuropilin signaling in a brain region-specific and cell type-specific manner. Collectively, the results indicate that similar to other ciliopathy-associated proteins, AC3 could be reasonably identified as a key player in associated ciliopathies, although why and how unique ciliary AC3-mediated cAMP signaling plays multiple functions across different brain areas and neuronal subtypes, including the infanticidal behaviors involved in the MOE, AON, and VMH regions, remain to be determined.

In summary, we reveal a new role for AC3, a ciliopathy-associated protein and demonstrate that its signaling in the MOE and in downstream brain regions, including the AON and VMH, is needed for the infanticidal behavior of adult virgin male mice. Our results expand the emerging roles of AC3 as a key player in ciliopathy-associated disorders. Because AC3 is widely expressed in brain areas and exclusively in the neuronal cilium, the mechanical insights obtained in this study should have broad implications beyond the infanticidal behavior in adult virgin male mice.

Limitations of the study

Although we discovered that targeted knockdown of AC3 in the MOE, AON, or VMH led to impaired infanticidal behavior in adult virgin male mice, we did not explore the mechanism underlying the involvement of ciliopathy-associated AC3 signaling in infanticide. How does AC3 on cilia transduce olfactory signals in the AON and VMH? AC3 was knocked down in the AON and VMH by a vector expressing AC3 shRNA driven by the U6 promoter, so we were unable to identify the neuronal subtypes in which AC3 plays a role in infanticide.

STAR★METHODS

Detailed methods are provided in the online version of this paper and include the following:

- KEY RESOURCES TABLE
- RESOURCE AVAILABILITY
  - Lead contact
  - Materials availability
  - Data and code availability
- EXPERIMENTAL MODEL AND SUBJECT DETAILS
  - Experimental animals
- METHOD DETAILS
  - AAV vector packaging
  - Nasal perfusion of 5% $ZnSO_4$ or AAV
  - Stereotactic injection of NMDA/NMLA and AAV
  - Behavioral assays
  - Spontaneous locomotor activity test
  - Odorant habituation/dishabituation assay
  - Resident/intruder experiment
  - Male mating behavior test
  - Infanticidal behavior test
  - Urine preference assay
  - RNA isolation and qPCR analyses
  - Tissue processing and IF
  - C-Fos IF
  - WB analysis
- QUANTIFICATION AND STATISTICAL ANALYSIS
  - Statistical analysis

SUPPLEMENTAL INFORMATION

Supplemental information can be found online at https://doi.org/10.1016/j.isci.2022.104534.

ACKNOWLEDGMENTS

We thank Drs. Anan Li and Jianxu Zhang, as well as the anonymous referees, for providing many constructive comments on the manuscript. We thank Mingshen Guo for the technical assistance with the imaging; the Fuqiang Xu Lab at the Wuhan Institute of Physics and Mathematics, Chinese Academy of Sciences, for the technical assistance with the stereotactic injection; and Hongxin Zhang and Haichen Lian for the routine animal husbandry. This work was supported by the National Natural Science Foundation of China (32070567 and 31871246); the Natural Science Foundation of Hebei Province of China (C2020201013); the Institute of Life Science and Green Development, Hebei University (050001–5000019); and the Excellent PhD Training Project of Hebei University (to DY).

AUTHOR CONTRIBUTIONS

Z.W., X. W., and D.Y. designed the experiments. X. W., D.Y., and Y. Z. performed the experiments. X. W., D.Y., and S. L. analyzed the data. All the authors discussed the results. Z.W. and X. W. wrote the manuscript. All the authors have read and approved the final version of the manuscript.

DECLARATION OF INTERESTS

The authors declare no competing financial interests.

Received: October 29, 2021
Revised: February 11, 2022
Accepted: June 1, 2022
Published: July 15, 2022

REFERENCES

Amano, T., Shindo, S., Yoshihara, C., Tsuneoka, Y., Uki, H., Minami, M., and Kuroda, K.O. (2017). Development-dependent behavioral change toward pups and synaptic transmission in the rhomboid nucleus of the bed nucleus of the stria terminalis. Behav. Brain Res. *325*, 131–137. https://doi.org/10.1016/j.bbr.2016.10.029.

Anvarian, Z., Mykytyn, K., Mukhopadhyay, S., Pedersen, L.B., and Christensen, S.T. (2019). Cellular signalling by primary cilia in development, organ function and disease. Nat. Rev. Nephrol. *15*, 199–219. https://doi.org/10.1038/s41581-019-0116-9.

Aqrabawi, A.J., Browne, C.J., Dargaei, Z., Garand, D., Khademullah, C.S., Woodin, M.A., and Kim, J.C. (2016). Top-down modulation of olfactory-guided behaviours by the anterior olfactory nucleus pars medialis and ventral hippocampus. Nat. Commun. *7*, 13721. https://doi.org/10.1038/ncomms13721.

Assous, M., Martinez, E., Eisenberg, C., Shah, F., Kosc, A., Varghese, K., Espinoza, D., Bhimani, S., Tepper, J.M., Shiflett, M.W., and Tran, T.S. (2019). Neuropilin 2 signaling mediates corticostriatal transmission, spine maintenance, and goal-directed learning in mice. J. Neurosci. *39*, 8845–8859. https://doi.org/10.1523/JNEUROSCI.1006-19.2019.

Autry, A.E., Wu, Z., Kapoor, V., Kohl, J., Bambah-Mukku, D., Rubinstein, N.D., Marin-Rodriguez, B., Carta, I., Sedwick, V., Tang, M., and Dulac, C. (2021). Urocortin-3 neurons in the mouse perifornical area promote infant-directed neglect and aggression. Elife *10*, e64680. https://doi.org/10.7554/eLife.64680.

Baum, M.J., and Cherry, J.A. (2015). Processing by the main olfactory system of chemosignals that facilitate mammalian reproduction. Horm. Behav. *68*, 53–64. https://doi.org/10.1016/j.yhbeh.2014.06.003.

Bayless, D.W., Yang, T., Mason, M.M., Susanto, A.A.T., Lobdell, A., and Shah, N.M. (2019). Limbic neurons shape sex recognition and social behavior in sexually naive males. Cell *176*, 1190–1205.e20. https://doi.org/10.1016/j.cell.2018.12.041.

Belluscio, L., Gold, G.H., Nemes, A., and Axel, R. (1998). Mice deficient in G(olf) are anosmic. Neuron *20*, 69–81. https://doi.org/10.1016/s0896-6273(00)80435-3.

Ben-Shaul, Y., Katz, L.C., Mooney, R., and Dulac, C. (2010). In vivo vomeronasal stimulation reveals sensory encoding of conspecific and allospecific cues by the mouse accessory olfactory bulb. Proc. Natl. Acad. Sci. USA *107*, 5172–5177. https://doi.org/10.1073/pnas.0915147107.

Beny-Shefer, Y., Zilkha, N., Lavi-Avnon, Y., Bezalel, N., Rogachev, I., Brandis, A., Dayan, M., and Kimchi, T. (2017). Nucleus accumbens dopamine signaling regulates sexual preference for females in male mice. Cell Rep. *21*, 3079–3088. https://doi.org/10.1016/j.celrep.2017.11.062.

Bergan, J.F., Ben-Shaul, Y., and Dulac, C. (2014). Sex-specific processing of social cues in the medial amygdala. Elife *3*, e02743. https://doi.org/10.7554/eLife.02743.

Bishop, G.A., Berbari, N.F., Lewis, J., and Mykytyn, K. (2007). Type III adenylyl cyclase localizes to primary cilia throughout the adult mouse brain. J. Comp. Neurol. *505*, 562–571. https://doi.org/10.1002/cne.21510.

Bleymehl, K., Pérez-Gómez, A., Omura, M., Moreno-Pérez, A., Macías, D., Bai, Z., Johnson, R.S., Leinders-Zufall, T., Zufall, F., and Mombaerts, P. (2016). A sensor for low environmental oxygen in the mouse main olfactory epithelium. Neuron *92*, 1196–1203. https://doi.org/10.1016/j.neuron.2016.11.001.

Boehm, U., Zou, Z., and Buck, L.B. (2005). Feedback loops link odor and pheromone signaling with reproduction. Cell *123*, 683–695. https://doi.org/10.1016/j.cell.2005.09.027.

Bowie, E., and Goetz, S.C. (2020). TTBK2 and primary cilia are essential for the connectivity and survival of cerebellar Purkinje neurons. Elife *9*, e51166. https://doi.org/10.7554/eLife.51166.

Brunet, L.J., Gold, G.H., and Ngai, J. (1996). General anosmia caused by a targeted disruption of the mouse olfactory cyclic nucleotide-gated cation channel. Neuron *17*, 681–693. https://doi.org/10.1016/s0896-6273(00)80200-7.

Cai, E., Zhang, J., and Ge, X. (2021). Control of the Hedgehog pathway by compartmentalized PKA in the primary cilium. Sci. China Life Sci. *65*, 500–514. https://doi.org/10.1007/s11427-021-1975-9.

Cariboni, A., Hickok, J., Rakic, S., Andrews, W., Maggi, R., Tischkau, S., and Parnavelas, J.G. (2007). Neuropilins and their ligands are important in the migration of gonadotropin-releasing hormone neurons. J. Neurosci. *27*, 2387–2395. https://doi.org/10.1523/JNEUROSCI.5075-06.2007.

Challis, R.C., Tian, H., Wang, J., He, J., Jiang, J., Chen, X., Yin, W., Connelly, T., Ma, L., Yu, C.R., et al. (2015). An olfactory cilia pattern in the mammalian nose ensures high sensitivity to odors. Curr. Biol. *25*, 2503–2512. https://doi.org/10.1016/j.cub.2015.07.065.

Chen, A.X., Yan, J.J., Zhang, W., Wang, L., Yu, Z.X., Ding, X.J., Wang, D.Y., Zhang, M., Zhang, Y.L., Song, N., et al. (2020). Specific hypothalamic neurons required for sensing conspecific male cues relevant to inter-male aggression. Neuron *108*, 763–774.e6. https://doi.org/10.1016/j.neuron.2020.08.025.

Chen, P.B., Hu, R.K., Wu, Y.E., Pan, L., Huang, S., Micevych, P.E., and Hong, W. (2019). Sexually dimorphic control of parenting behavior by the medial amygdala. Cell *176*, 1206–1221.e18. https://doi.org/10.1016/j.cell.2019.01.024.

Chen, X., Luo, J., Leng, Y., Yang, Y., Zweifel, L.S., Palmiter, R.D., and Storm, D.R. (2016). Ablation of type III adenylyl cyclase in mice causes reduced neuronal activity, altered sleep pattern, and depression-like phenotypes. Biol Psychiatry *80*, 836–848. https://doi.org/10.1016/j.biopsych.2015.12.012.

Chesler, A.T., Zou, D.J., Le Pichon, C.E., Peterlin, Z.A., Matthews, G.A., Pei, X., Miller, M.C., and Firestein, S. (2007). A G protein/cAMP signal cascade is required for axonal convergence into olfactory glomeruli. Proc. Natl. Acad. Sci. USA *104*, 1039–1044. https://doi.org/10.1073/pnas.0609215104.

Choi, G.B., Dong, H.W., Murphy, A.J., Valenzuela, D.M., Yancopoulos, G.D., Swanson, L.W., and Anderson, D.J. (2005). Lhx6 delineates a pathway mediating innate reproductive behaviors from the amygdala to the hypothalamus. Neuron *46*, 647–660. https://doi.org/10.1016/j.neuron.2005.04.011.

Col, J.A.D., Matsuo, T., Storm, D.R., and Rodriguez, I. (2007). Adenylyl cyclase-dependent axonal targeting in the olfactory system. Development *134*, 2481–2489. https://doi.org/10.1242/dev.006346.

Demyanenko, G.P., Mohan, V., Zhang, X., Brennaman, L.H., Dharbal, K.E.S., Tran, T.S., Manis, P.B., and Maness, P.F. (2014). Neural cell adhesion molecule NrCAM regulates Semaphorin 3F-induced dendritic spine remodeling. J. Neurosci. *34*, 11274–11287. https://doi.org/10.1523/JNEUROSCI.1774-14.2014.

Dhungel, S., Masaoka, M., Rai, D., Kondo, Y., and Sakuma, Y. (2011). Both olfactory epithelial and vomeronasal inputs are essential for activation of the medial amygdala and preoptic neurons of male rats. Neuroscience *199*, 225–234. https://doi.org/10.1016/j.neuroscience.2011.09.051.

Dimén, D., Puska, G., Szendi, V., Sipos, E., Zelena, D., and Dobolyi, Á. (2021). Sex-specific parenting and depression evoked by preoptic inhibitory neurons. iScience *24*, 103090. https://doi.org/10.1016/j.isci.2021.103090.

Duncan, B.W., Mohan, V., Wade, S.D., Truong, Y., Kampov-Polevoi, A., Temple, B.R., and Maness, P.F. (2021). Semaphorin3F drives dendritic spine pruning through rho-GTPase signaling. Mol. Neurobiol. *58*, 3817–3834. https://doi.org/10.1007/s12035-021-02373-2.

Farbman, A.I., and Margolis, F.L. (1980). Olfactory marker protein during ontogeny: immunohistochemical localization. Dev. Biol. *74*, 205–215. https://doi.org/10.1016/0012-1606(80)90062-7.

Frattarelli, J.L., Krsmanovic, L.Z., and Catt, K.J. (2011). The relationship between pulsatile GnRH secretion and cAMP production in immortalized GnRH neurons. Am. J. Physiol. Endocrinol. Metab. *300*, E1022–E1030. https://doi.org/10.1152/ajpendo.00081.2011.

Fukui, K., Sato, K., Murakawa, S., Minami, M., and Amano, T. (2022). Estrogen signaling modulates behavioral selection toward pups and amygdalohippocampal area in the rhomboid nucleus of the bed nucleus of the stria terminalis circuit. Neuropharmacology *204*, 108879. https://doi.org/10.1016/j.neuropharm.2021.108879.

Gipson, C.D., and Olive, M.F. (2017). Structural and functional plasticity of dendritic spines - root or result of behavior? Gene Brain Behav. *16*, 101–117. https://doi.org/10.1111/gbb.12324.

Green, W.W., Uytingco, C.R., Ukhanov, K., Kolb, Z., Moretta, J., McIntyre, J.C., and Martens, J.R. (2018). Peripheral gene therapeutic rescue of an olfactory ciliopathy restores sensory input, axonal pathfinding, and odor-guided behavior. J. Neurosci. *38*, 7462–7475. https://doi.org/10.1523/JNEUROSCI.0084-18.2018.

Guadiana, S.M., Semple-Rowland, S., Daroszewski, D., Madorsky, I., Breunig, J.J., Mykytyn, K., and Sarkisian, M.R. (2013). Arborization of dendrites by developing neocortical neurons is dependent on primary cilia and type 3 adenylyl cyclase. J. Neurosci. *33*, 2626–2638. https://doi.org/10.1523/JNEUROSCI.2906-12.2013.

Guemez-Gamboa, A., Coufal, N.G., and Gleeson, J.G. (2014). Primary cilia in the developing and mature brain. Neuron *82*, 511–521. https://doi.org/10.1016/j.neuron.2014.04.024.

Guo, J., Otis, J.M., Higginbotham, H., Monckton, C., Cheng, J., Asokan, A., Mykytyn, K., Caspary, T., Stuber, G.D., and Anton, E.S. (2017). Primary cilia signaling shapes the development of interneuronal connectivity. Dev. Cell *42*, 286–300.e4. https://doi.org/10.1016/j.devcel.2017.07.010.

Guo, J., Otis, J.M., Suciu, S.K., Catalano, C., Xing, L., Constable, S., Wachten, D., Gupton, S., Lee, J., Lee, A., et al. (2019). Primary cilia signaling promotes axonal tract development and is disrupted in joubert syndrome-related disorders models. Dev. Cell *51*, 759–774.e5. https://doi.org/10.1016/j.devcel.2019.11.005.

Halem, H.A., Cherry, J.A., and Baum, M.J. (1999). Vomeronasal neuroepithelium and forebrain Fos responses to male pheromones in male and female mice. J. Neurobiol. *39*, 249–263. https://doi.org/10.1002/(sici)1097-4695(199905)39:2<249::aid-neu9>3.0.co;2-r.

Haq, N., Schmidt-Hieber, C., Sialana, F.J., Ciani, L., Heller, J.P., Stewart, M., Bentley, L., Wells, S., Rodenburg, R.J., Nolan, P.M., et al. (2019). Loss of Bardet-Biedl syndrome proteins causes synaptic aberrations in principle neurons. PLoS Biol. *17*, e3000414. https://doi.org/10.1371/journal.pbio.3000414.

Henion, T.R., Faden, A.A., Knott, T.K., and Schwarting, G.A. (2011). β3GnT2 maintains adenylyl cyclase-3 signaling and axon guidance molecule expression in the olfactory epithelium. J. Neurosci. *31*, 6576–6586. https://doi.org/10.1523/JNEUROSCI.0224-11.2011.

Hildebrandt, F., Benzing, T., and Katsanis, N. (2011). Ciliopathies. N. Engl. J. Med. *364*, 1533–1543. https://doi.org/10.1056/NEJMra1010172.

Hillman, R.T., Feng, B.Y., Ni, J., Woo, W.M., Milenkovic, L., Hayden Gephart, M.G., Teruel, M.N., Oro, A.E., Chen, J.K., and Scott, M.P. (2011). Neuropilins are positive regulators of Hedgehog signal transduction. Genes Dev. *25*, 2333–2346. https://doi.org/10.1101/gad.173054.111.

Imai, T., Yamazaki, T., Kobayakawa, R., Kobayakawa, K., Abe, T., Suzuki, M., and Sakano, H. (2009). Pre-target axon sorting establishes the neural map topography. Science *325*, 585–590. https://doi.org/10.1126/science.1173596.

Inbar, T., Davis, R., and Bergan, J.F. (2022). A sex-specific feedback projection from aromatase-expressing neurons in the medial amygdala to the accessory olfactory bulb. J. Comp. Neurol. *530*, 648–655. https://doi.org/10.1002/cne.25236.

Inokuchi, K., Imamura, F., Takeuchi, H., Kim, R., Okuno, H., Nishizumi, H., Bito, H., Kikusui, T., and Sakano, H. (2017). Nrp2 is sufficient to instruct circuit formation of mitral-cells to mediate odour-induced attractive social responses. Nat. Commun. *8*, 15977. https://doi.org/10.1038/ncomms15977.

Ishii, K.K., Osakada, T., Mori, H., Miyasaka, N., Yoshihara, Y., Miyamichi, K., and Touhara, K. (2017). A labeled-line neural circuit for pheromone-mediated sexual behaviors in mice. Neuron *95*, 123–137.e8. https://doi.org/10.1016/j.neuron.2017.05.038.

Isogai, Y., Wu, Z., Love, M.I., Ahn, M.H.Y., Bambah-Mukku, D., Hua, V., Farrell, K., and Dulac, C. (2018). Multisensory logic of infant-directed aggression by males. Cell *175*, 1827–1841.e17. https://doi.org/10.1016/j.cell.2018.11.032.

Jakupovic, J., Kang, N., and Baum, M.J. (2008). Effect of bilateral accessory olfactory bulb lesions on volatile urinary odor discrimination and investigation as well as mating behavior in male mice. Physiol. Behav. *93*, 467–473. https://doi.org/10.1016/j.physbeh.2007.10.005.

Kang, N., Baum, M.J., and Cherry, J.A. (2009). A direct main olfactory bulb projection to the 'vomeronasal' amygdala in female mice selectively responds to volatile pheromones from males. Eur. J. Neurosci. *29*, 624–634. https://doi.org/10.1111/j.1460-9568.2009.06638.x.

Kang, N., McCarthy, E.A., Cherry, J.A., and Baum, M.J. (2011). A sex comparison of the anatomy and function of the main olfactory bulb-medial amygdala projection in mice. Neuroscience *172*, 196–204. https://doi.org/10.1016/j.neuroscience.2010.11.003.

Keshavarzi, S., Power, J.M., Albers, E.H.H., Sullivan, R.K., and Sah, P. (2015). Dendritic organization of olfactory inputs to medial amygdala neurons. J. Neurosci. *35*, 13020–13028. https://doi.org/10.1523/JNEUROSCI.0627-15.2015.

Kohl, J. (2020). Parenting - a paradigm for investigating the neural circuit basis of behavior. Curr. Opin. Neurobiol. *60*, 84–91. https://doi.org/10.1016/j.conb.2019.11.011.

Kohl, J., Autry, A.E., and Dulac, C. (2017). The neurobiology of parenting: a neural circuit perspective. Bioessays *39*, e201600159. https://doi.org/10.1002/bies.201600159.

Koike, K., Yoo, S.J., Bleymehl, K., Omura, M., Zapiec, B., Pyrski, M., Blum, T., Khan, M., Bai, Z., Leinders-Zufall, T., et al. (2021). Danger perception and stress response through an olfactory sensor for the bacterial metabolite hydrogen sulfide. Neuron *109*, 2469–2484.e7. https://doi.org/10.1016/j.neuron.2021.05.032.

Korzan, W.J., Freamat, M., Johnson, A.G., Cherry, J.A., and Baum, M.J. (2013). Either main or accessory olfactory system signaling can mediate the rewarding effects of estrous female chemosignals in sexually naive male mice. Behav. Neurosci. *127*, 755–762. https://doi.org/10.1037/a0033945.

Kulkarni, V.A., and Firestein, B.L. (2012). The dendritic tree and brain disorders. Mol. Cell. Neurosci. *50*, 10–20. https://doi.org/10.1016/j.mcn.2012.03.005.

Kumamoto, N., Gu, Y., Wang, J., Janoschka, S., Takemaru, K.I., Levine, J., and Ge, S. (2012). A role for primary cilia in glutamatergic synaptic integration of adult-born neurons. Nat. Neurosci. *15*, 399–405.S91. https://doi.org/10.1038/nn.3042.

Lee, C.H., Song, D.K., Park, C.B., Choi, J., Kang, G.M., Shin, S.H., Kwon, I., Park, S., Kim, S., Kim, J.Y., et al. (2020). Primary cilia mediate early life programming of adiposity through lysosomal regulation in the developing mouse hypothalamus. Nat. Commun. *11*, 5772. https://doi.org/10.1038/s41467-020-19638-4.

Lemons, K., Fu, Z., Aoudé, I., Ogura, T., Sun, J., Chang, J., Mbonu, K., Matsumoto, I., Arakawa, H.,

and Lin, W. (2017). Lack of TRPM5-expressing microvillous cells in mouse main olfactory epithelium leads to impaired odor-evoked responses and olfactory-guided behavior in a challenging chemical environment. eNeuro *4*. https://doi.org/10.1523/eneuro.0135-17.2017.

Li, M., Masugi-Tokita, M., Takanami, K., Yamada, S., and Kawata, M. (2012). Testosterone has sublayer-specific effects on dendritic spine maturation mediated by BDNF and PSD-95 in pyramidal neurons in the hippocampus CA1 area. Brain Res. *1484*, 76–84. https://doi.org/10.1016/j.brainres.2012.09.028.

Li, Z., Jagadapillai, R., Gozal, E., and Barnes, G. (2019). Deletion of semaphorin 3F in interneurons is associated with decreased GABAergic neurons, autism-like behavior, and increased oxidative stress cascades. Mol. Neurobiol. *56*, 5520–5538. https://doi.org/10.1007/s12035-018-1450-9.

Liberles, S.D. (2014). Mammalian pheromones. Annu. Rev. Physiol. *76*, 151–175. https://doi.org/10.1146/annurev-physiol-021113-170334.

Liu, X., Zhou, Y., Li, S., Yang, D., Jiao, M., Liu, X., and Wang, Z. (2020a). Type 3 adenylyl cyclase in the main olfactory epithelium participates in depression-like and anxiety-like behaviours. J. Affect. Disord. *268*, 28–38. https://doi.org/10.1016/j.jad.2020.02.041.

Liu, X., Zhou, Y., Yang, D., Li, S., Liu, X., and Wang, Z. (2020b). Type 3 adenylyl cyclase in the MOE is involved in learning and memory in mice. Behav. Brain Res. *383*, 112533. https://doi.org/10.1016/j.bbr.2020.112533.

Livera, G., Xie, F., Garcia, M.A., Jaiswal, B., Chen, J., Law, E., Storm, D.R., and Conti, M. (2005). Inactivation of the mouse adenylyl cyclase 3 gene disrupts male fertility and spermatozoon function. Mol. Endocrinol. *19*, 1277–1290. https://doi.org/10.1210/me.2004-0318.

Lo, L., Yao, S., Kim, D.W., Cetin, A., Harris, J., Zeng, H., Anderson, D.J., and Weissbourd, B. (2019). Connectional architecture of a mouse hypothalamic circuit node controlling social behavior. Proc. Natl. Acad. Sci. USA *116*, 7503–7512. https://doi.org/10.1073/pnas.1817503116.

Loktev, A.V., and Jackson, P.K. (2013). Neuropeptide Y family receptors traffic via the Bardet-Biedl syndrome pathway to signal in neuronal primary cilia. Cell Rep. *5*, 1316–1329. https://doi.org/10.1016/j.celrep.2013.11.011.

Lukas, D., and Huchard, E. (2014). The evolution of infanticide by males in mammalian societies. Science *346*, 841–844. https://doi.org/10.1126/science.1257226.

Maden, C.H., Gomes, J., Schwarz, Q., Davidson, K., Tinker, A., and Ruhrberg, C. (2012). NRP1 and NRP2 cooperate to regulate gangliogenesis, axon guidance and target innervation in the sympathetic nervous system. Dev. Biol. *369*, 277–285. https://doi.org/10.1016/j.ydbio.2012.06.026.

Martel, K.L., and Baum, M.J. (2009). Adult testosterone treatment but not surgical disruption of vomeronasal function augments male-typical sexual behavior in female mice. J. Neurosci. *29*, 7658–7666. https://doi.org/10.1523/JNEUROSCI.1311-09.2009.

Martínez-García, F., Martínez-Ricós, J., Agustín-Pavón, C., Martínez-Hernández, J., Novejarque, A., and Lanuza, E. (2009). Refining the dual olfactory hypothesis: pheromone reward and odour experience. Behav. Brain Res. *200*, 277–286. https://doi.org/10.1016/j.bbr.2008.10.002.

Martínez, A., Ramos, G., Martínez-Torres, M., Nicolás, L., Carmona, A., Cárdenas, M., and Luis, J. (2015). Paternal behavior in the Mongolian gerbil (Meriones unguiculatus): estrogenic and androgenic regulation. Horm. Behav. *71*, 91–95. https://doi.org/10.1016/j.yhbeh.2015.04.009.

Matsuo, T., Hattori, T., Asaba, A., Inoue, N., Kanomata, N., Kikusui, T., Kobayakawa, R., and Kobayakawa, K. (2015). Genetic dissection of pheromone processing reveals main olfactory system-mediated social behaviors in mice. Proc. Natl. Acad. Sci. USA *112*, E311–E320. https://doi.org/10.1073/pnas.1416723112.

McCarthy, M.M., and vom Saal, F.S. (1985). The influence of reproductive state on infanticide by wild female house mice (Mus musculus). Physiol. Behav. *35*, 843–849. https://doi.org/10.1016/0031-9384(85)90248-3.

McCarthy, M.M., and vom Saal, F.S. (1986a). Infanticide by virgin CF-1 and wild male house mice (Mus musculus): effects of age, prolonged isolation, and testing procedure. Dev. Psychobiol. *19*, 279–290. https://doi.org/10.1002/dev.420190313.

McCarthy, M.M., and vom Saal, F.S. (1986b). Inhibition of infanticide after mating by wild male house mice. Physiol. Behav. *36*, 203–209. https://doi.org/10.1016/0031-9384(86)90004-1.

Menco, B.P. (1997). Ultrastructural aspects of olfactory signaling. Chem. Senses *22*, 295–311. https://doi.org/10.1093/chemse/22.3.295.

Mennella, J.A., and Moltz, H. (1988). Infanticide in the male rat: the role of the vomeronasal organ. Physiol. Behav. *42*, 303–306. https://doi.org/10.1016/0031-9384(88)90087-x.

Meredith, M., Marques, D.M., O'Connell, R.J., and Stern, F.L. (1980). Vomeronasal pump: significance for male hamster sexual behavior. Science *207*, 1224–1226. https://doi.org/10.1126/science.7355286.

Meredith, M., and O'Connell, R.J. (1979). Efferent control of stimulus access to the hamster vomeronasal organ. J. Physiol. *286*, 301–316. https://doi.org/10.1113/jphysiol.1979.sp012620.

Messina, A., Langlet, F., Chachlaki, K., Roa, J., Rasika, S., Jouy, N., Gallet, S., Gaytan, F., Parkash, J., Tena-Sempere, M., et al. (2016). A microRNA switch regulates the rise in hypothalamic GnRH production before puberty. Nat. Neurosci. *19*, 835–844. https://doi.org/10.1038/nn.4298.

Mohan, V., Sullivan, C.S., Guo, J., Wade, S.D., Majumder, S., Agarwal, A., Anton, E.S., Temple, B.S., and Maness, P.F. (2019). Temporal regulation of dendritic spines through NrCAM-semaphorin3F receptor signaling in developing cortical pyramidal neurons. Cereb. Cortex *29*, 963–977. https://doi.org/10.1093/cercor/bhy004.

Mohan, V., Wyatt, E.V., Gotthard, I., Phend, K.D., Diestel, S., Duncan, B.W., Weinberg, R.J., Tripathy, A., and Maness, P.F. (2018). Neurocan inhibits semaphorin 3F induced dendritic spine remodeling through NrCAM in cortical neurons. Front. Cell. Neurosci. *12*, 346. https://doi.org/10.3389/fncel.2018.00346.

Mori, K., and Sakano, H. (2021). Olfactory circuitry and behavioral decisions. Annu. Rev. Physiol. *83*, 231–256. https://doi.org/10.1146/annurev-physiol-031820-092824.

Mucignat-Caretta, C. (2021). Processing of intraspecific chemical signals in the rodent brain. Cell Tissue Res. *383*, 525–533. https://doi.org/10.1007/s00441-020-03383-7.

Numan, M., Corodimas, K.P., Numan, M.J., Factor, E.M., and Piers, W.D. (1988). Axon-sparing lesions of the preoptic region and substantia innominata disrupt maternal behavior in rats. Behav. Neurosci. *102*, 381–396. https://doi.org/10.1037//0735-7044.102.3.381.

Omura, M., and Mombaerts, P. (2015). Trpc2-expressing sensory neurons in the mouse main olfactory epithelium of type B express the soluble guanylate cyclase Gucy1b2. Mol. Cell. Neurosci. *65*, 114–124. https://doi.org/10.1016/j.mcn.2015.02.012.

Pandolfi, E.C., Hoffmann, H.M., Schoeller, E.L., Gorman, M.R., and Mellon, P.L. (2018). Haploinsufficiency of SIX3 abolishes male reproductive behavior through disrupted olfactory development, and impairs female fertility through disrupted GnRH neuron migration. Mol. Neurobiol. *55*, 8709–8727. https://doi.org/10.1007/s12035-018-1013-0.

Pankevich, D.E., Baum, M.J., and Cherry, J.A. (2004). Olfactory sex discrimination persists, whereas the preference for urinary odorants from estrous females disappears in male mice after vomeronasal organ removal. J. Neurosci. *24*, 9451–9457. https://doi.org/10.1523/JNEUROSCI.2376-04.2004.

Pankevich, D.E., Cherry, J.A., and Baum, M.J. (2006). Effect of vomeronasal organ removal from male mice on their preference for and neural fos responses to female urinary odors. Behav. Neurosci. *120*, 925–936. https://doi.org/10.1037/0735-7044.120.4.925.

Parisi, M.A. (2019). The molecular genetics of Joubert syndrome and related ciliopathies: the challenges of genetic and phenotypic heterogeneity. Transl. Sci. Rare Dis. *4*, 25–49. https://doi.org/10.3233/TRD-190041.

Paxinos, G. (2004). The Rat Nervous System (Elsevier Academic).

Pérez-Gómez, A., Bleymehl, K., Stein, B., Pyrski, M., Birnbaumer, L., Munger, S.D., Leinders-Zufall, T., Zufall, F., and Chamero, P. (2015). Innate predator odor aversion driven by parallel olfactory subsystems that converge in the ventromedial hypothalamus. Curr. Biol. *25*, 1340–1346. https://doi.org/10.1016/j.cub.2015.03.026.

Pinskey, J.M., Franks, N.E., McMellen, A.N., Giger, R.J., and Allen, B.L. (2017). Neuropilin-1 promotes Hedgehog signaling through a novel cytoplasmic motif. J. Biol. Chem. *292*, 15192–15204. https://doi.org/10.1074/jbc.M117.783845.

Pro-Sistiaga, P., Mohedano-Moriano, A., Ubeda-Bañon, I., Del Mar Arroyo-Jimenez, M., Marcos, P., Artacho-Pérula, E., Crespo, C., Insausti, R., and

Martinez-Marcos, A. (2007). Convergence of olfactory and vomeronasal projections in the rat basal telencephalon. J. Comp. Neurol. *504*, 346–362. https://doi.org/10.1002/cne.21455.

Raam, T., and Hong, W. (2021). Organization of neural circuits underlying social behavior: a consideration of the medial amygdala. Curr. Opin. Neurobiol. *68*, 124–136. https://doi.org/10.1016/j.conb.2021.02.008.

Reiter, J.F., and Leroux, M.R. (2017). Genes and molecular pathways underpinning ciliopathies. Nat. Rev. Mol. Cell Biol. *18*, 533–547. https://doi.org/10.1038/nrm.2017.60.

Riccomagno, M.M., Hurtado, A., Wang, H., Macopson, J.G., Griner, E.M., Betz, A., Brose, N., Kazanietz, M.G., and Kolodkin, A.L. (2012). The RacGAP β2-chimaerin selectively mediates axonal pruning in the Hippocampus. Cell *149*, 1594–1606. https://doi.org/10.1016/j.cell.2012.05.018.

Romero-Morales, L., García-Saucedo, B., Martínez-Torres, M., Cárdenas-Vázquez, R., Álvarez-Rodríguez, C., Carmona, A., and Luis, J. (2021). Paternal and infanticidal behavior in the Mongolian gerbil (Meriones unguiculatus): an approach to neuroendocrine regulation. Behav. Brain Res. *415*, 113520. https://doi.org/10.1016/j.bbr.2021.113520.

Sarkisian, M.R., and Guadiana, S.M. (2015). Influences of primary cilia on cortical morphogenesis and neuronal subtype maturation. Neuroscientist *21*, 136–151. https://doi.org/10.1177/1073858414531074.

Sato, K., Hamasaki, Y., Fukui, K., Ito, K., Miyamichi, K., Minami, M., and Amano, T. (2020). Amygdalohippocampal area neurons that project to the preoptic area mediate infant-directed attack in male mice. J. Neurosci. *40*, 3981–3994. https://doi.org/10.1523/JNEUROSCI.0438-19.2020.

Schwarting, G.A., and Henion, T.R. (2011). Regulation and function of axon guidance and adhesion molecules during olfactory map formation. J. Cell. Biochem. *112*, 2663–2671. https://doi.org/10.1002/jcb.23203.

Shao, Y.F., Wang, C., Rao, X.P., Wang, H.D., Ren, Y.L., Li, J., Dong, C.Y., Xie, J.F., Yang, X.W., Xu, F.Q., and Hou, Y.P. (2021). Neuropeptide S attenuates the alarm pheromone-evoked defensive and risk assessment behaviors through activation of cognate receptor-expressing neurons in the posterior medial amygdala. Front. Mol. Neurosci. *14*, 752516. https://doi.org/10.3389/fnmol.2021.752516.

Siljee, J.E., Wang, Y., Bernard, A.A., Ersoy, B.A., Zhang, S., Marley, A., Von Zastrow, M., Reiter, J.F., and Vaisse, C. (2018). Subcellular localization of MC4R with ADCY3 at neuronal primary cilia underlies a common pathway for genetic predisposition to obesity. Nat. Genet. *50*, 180–185. https://doi.org/10.1038/s41588-017-0020-9.

Sipos, É., Komoly, S., and Acs, P. (2018). Quantitative comparison of primary cilia marker expression and length in the mouse brain. J. Mol. Neurosci. *64*, 397–409. https://doi.org/10.1007/s12031-018-1036-z.

Slotnick, B., Restrepo, D., Schellinck, H., Archbold, G., Price, S., and Lin, W. (2010). Accessory olfactory bulb function is modulated by input from the main olfactory epithelium. Eur. J. Neurosci. *31*, 1108–1116. https://doi.org/10.1111/j.1460-9568.2010.07141.x.

Stagkourakis, S., Smiley, K.O., Williams, P., Kakadellis, S., Ziegler, K., Bakker, J., Brown, R.S.E., Harkany, T., Grattan, D.R., and Broberger, C. (2020). A neuro-hormonal circuit for paternal behavior controlled by a hypothalamic network oscillation. Cell *182*, 960–975.e15. https://doi.org/10.1016/j.cell.2020.07.007.

Stowers, L., and Kuo, T.H. (2015). Mammalian pheromones: emerging properties and mechanisms of detection. Curr. Opin. Neurobiol. *34*, 103–109. https://doi.org/10.1016/j.conb.2015.02.005.

Sun, Z., Wang, B., Chen, C., Li, C., and Zhang, Y. (2021). 5-HT6R null mutatrion induces synaptic and cognitive defects. Aging Cell *20*, e13369. https://doi.org/10.1111/acel.13369.

Swiech, L., Heidenreich, M., Banerjee, A., Habib, N., Li, Y., Trombetta, J., Sur, M., and Zhang, F. (2015). In vivo interrogation of gene function in the mammalian brain using CRISPR-Cas9. Nat. Biotechnol. *33*, 102–106. https://doi.org/10.1038/nbt.3055.

Tachikawa, K.S., Yoshihara, Y., and Kuroda, K.O. (2013). Behavioral transition from attack to parenting in male mice: a crucial role of the vomeronasal system. J. Neurosci. *33*, 5120–5126. https://doi.org/10.1523/JNEUROSCI.2364-12.2013.

Tan, C., Lu, N.N., Wang, C.K., Chen, D.Y., Sun, N.H., Lyu, H., Körbelin, J., Shi, W.X., Fukunaga, K., Lu, Y.M., and Han, F. (2019). Endothelium-derived semaphorin 3G regulates hippocampal synaptic structure and plasticity via neuropilin-2/PlexinA4. Neuron *101*, 920–937.e13. https://doi.org/10.1016/j.neuron.2018.12.036.

Tereshko, L., Gao, Y., Cary, B.A., Turrigiano, G.G., and Sengupta, P. (2021). Ciliary neuropeptidergic signaling dynamically regulates excitatory synapses in postnatal neocortical pyramidal neurons. Elife *10*, e65427. https://doi.org/10.7554/eLife.65427.

Thompson, J.A., Salcedo, E., Restrepo, D., and Finger, T.E. (2012). Second-order input to the medial amygdala from olfactory sensory neurons expressing the transduction channel TRPM5. J. Comp. Neurol. *520*, 1819–1830. https://doi.org/10.1002/cne.23015.

Tran, T.S., Rubio, M.E., Clem, R.L., Johnson, D., Case, L., Tessier-Lavigne, M., Huganir, R.L., Ginty, D.D., and Kolodkin, A.L. (2009). Secreted semaphorins control spine distribution and morphogenesis in the postnatal CNS. Nature *462*, 1065–1069. https://doi.org/10.1038/nature08628.

Trinh, K., and Storm, D.R. (2003). Vomeronasal organ detects odorants in absence of signaling through main olfactory epithelium. Nat. Neurosci. *6*, 519–525. https://doi.org/10.1038/nn1039.

Trouillet, A.C., Keller, M., Weiss, J., Leinders-Zufall, T., Birnbaumer, L., Zufall, F., and Chamero, P. (2019). Central role of G protein Gαi2 and Gαi2^{+} vomeronasal neurons in balancing territorial and infant-directed aggression of male mice. Proc. Natl. Acad. Sci. USA *116*, 5135–5143. https://doi.org/10.1073/pnas.1821492116.

Tsuneoka, Y., Tokita, K., Yoshihara, C., Amano, T., Esposito, G., Huang, A.J., Yu, L.M., Odaka, Y., Shinozuka, K., McHugh, T.J., and Kuroda, K.O. (2015). Distinct preoptic-BST nuclei dissociate paternal and infanticidal behavior in mice. EMBO J. *34*, 2652–2670. https://doi.org/10.15252/embj.201591942.

van der Klaauw, A.A., Croizier, S., Mendes de Oliveira, E., Stadler, L.K.J., Park, S., Kong, Y., Banton, M.C., Tandon, P., Hendricks, A.E., Keogh, J.M., et al. (2019). Human semaphorin 3 variants link melanocortin circuit development and energy balance. Cell *176*, 729–742.e18. https://doi.org/10.1016/j.cell.2018.12.009.

Vanacker, C., Trova, S., Shruti, S., Casoni, F., Messina, A., Croizier, S., Malone, S., Ternier, G., Hanchate, N.K., Rasika, S., et al. (2020). Neuropilin-1 expression in GnRH neurons regulates prepubertal weight gain and sexual attraction. EMBO J. *39*, e104633. https://doi.org/10.15252/embj.2020104633.

Vargas-Barroso, V., Ordaz-Sánchez, B., Peña-Ortega, F., and Larriva-Sahd, J.A. (2015). Electrophysiological evidence for a direct link between the main and accessory olfactory bulbs in the adult rat. Front. Neurosci. *9*, 518. https://doi.org/10.3389/fnins.2015.00518.

vom Saal, F.S., and Howard, L.S. (1982). The regulation of infanticide and parental behavior: implications for reproductive success in male mice. Science *215*, 1270–1272. https://doi.org/10.1126/science.7058349.

Wang, Z., Balet Sindreu, C., Li, V., Nudelman, A., Chan, G.C.K., and Storm, D.R. (2006). Pheromone detection in male mice depends on signaling through the type 3 adenylyl cyclase in the main olfactory epithelium. J. Neurosci. *26*, 7375–7379. https://doi.org/10.1523/JNEUROSCI.1967-06.2006.

Wang, Z., Li, V., Chan, G.C.K., Phan, T., Nudelman, A.S., Xia, Z., and Storm, D.R. (2009). Adult type 3 adenylyl cyclase-deficient mice are obese. PLoS One *4*, e6979. https://doi.org/10.1371/journal.pone.0006979.

Wang, Z., Nudelman, A., and Storm, D.R. (2007). Are pheromones detected through the main olfactory epithelium? Mol. Neurobiol. *35*, 317–323. https://doi.org/10.1007/s12035-007-0014-1.

Wang, Z., Phan, T., and Storm, D.R. (2011). The type 3 adenylyl cyclase is required for novel object learning and extinction of contextual memory: role of cAMP signaling in primary cilia. J. Neurosci. *31*, 5557–5561. https://doi.org/10.1523/JNEUROSCI.6561-10.2011.

Wang, Z., and Storm, D.R. (2011). Maternal behavior is impaired in female mice lacking type 3 adenylyl cyclase. Neuropsychopharmacology *36*, 772–781. https://doi.org/10.1038/npp.2010.211.

Wong, S.T., Trinh, K., Hacker, B., Chan, G.C., Lowe, G., Gaggar, A., Xia, Z., Gold, G.H., and Storm, D.R. (2000). Disruption of the type III adenylyl cyclase gene leads to peripheral and behavioral anosmia in transgenic mice. Neuron *27*, 487–497. https://doi.org/10.1016/s0896-6273(00)00060-x.

Woodley, S.K., Cloe, A.L., Waters, P., and Baum, M.J. (2004). Effects of vomeronasal organ removal on olfactory sex discrimination and odor preferences of female ferrets. Chem. Senses *29*, 659–669. https://doi.org/10.1093/chemse/bjh069.

Wu, Z., Autry, A.E., Bergan, J.F., Watabe-Uchida, M., and Dulac, C.G. (2014). Galanin neurons in the medial preoptic area govern parental behaviour. Nature *509*, 325–330. https://doi.org/10.1038/nature13307.

Yang, D., Wu, X., Wang, W., Zhou, Y., and Wang, Z. (2022). Ciliary type III adenylyl cyclase in the VMH is crucial for high-fat diet-induced obesity mediated by autophagy. Adv. Sci. *9*, e2102568. https://doi.org/10.1002/advs.202102568.

Yang, D., Wu, X., Zhou, Y., Wang, W., and Wang, Z. (2020). The microRNA/TET3/REST axis is required for olfactory globose basal cell proliferation and male behavior. EMBO Rep. *21*, e49431. https://doi.org/10.15252/embr.201949431.

Yang, X.Y., Ma, Z.L., Storm, D.R., Cao, H., and Zhang, Y.Q. (2021). Selective ablation of type 3 adenylyl cyclase in somatostatin-positive interneurons produces anxiety- and depression-like behaviors in mice. World J. Psychiatr. *11*, 35–49. https://doi.org/10.5498/wjp.v11.i2.35.

Yoon, H., Enquist, L.W., and Dulac, C. (2005). Olfactory inputs to hypothalamic neurons controlling reproduction and fertility. Cell *123*, 669–682. https://doi.org/10.1016/j.cell.2005.08.039.

Yoshihara, C., Tokita, K., Maruyama, T., Kaneko, M., Tsuneoka, Y., Fukumitsu, K., Miyazawa, E., Shinozuka, K., Huang, A.J., Nishimori, K., et al. (2021). Calcitonin receptor signaling in the medial preoptic area enables risk-taking maternal care. Cell Rep. *35*, 109204. https://doi.org/10.1016/j.celrep.2021.109204.

Zhang, Z., Yang, D., Zhang, M., Zhu, N., Zhou, Y., Storm, D.R., and Wang, Z. (2017). Deletion of type 3 adenylyl cyclase perturbs the postnatal maturation of olfactory sensory neurons and olfactory cilium ultrastructure in mice. Front. Cell. Neurosci. *11*, 1. https://doi.org/10.3389/fncel.2017.00001.

Zhou, K., Zhou, Y., Yang, D., Chen, T., Liu, X., Li, S., and Wang, Z. (2021). The type 3 adenylyl cyclase is crucial for intestinal mucosal neural network in the gut lamina propria. Neuro Gastroenterol. Motil. *33*, e14140. https://doi.org/10.1111/nmo.14140.

Zou, D.J., Chesler, A.T., Le Pichon, C.E., Kuznetsov, A., Pei, X., Hwang, E.L., and Firestein, S. (2007). Absence of adenylyl cyclase 3 perturbs peripheral olfactory projections in mice. J. Neurosci. *27*, 6675–6683. https://doi.org/10.1523/JNEUROSCI.0699-07.2007.

STAR★METHODS

KEY RESOURCES TABLE

REAGENT or RESOURCE	SOURCE	IDENTIFIER
Antibodies		
Rabbit Anti-Adenylate Cyclase 3, use 1:1,000 for IF	Novus	Cat#NBP1-92683SS; RRID: AB_11028381
Rabbit Anti-beta III Tubulin, use 1:500 for IF	Abcam	Cat#ab18207; RRID: AB_444319
Goat Anti-OMP, use 1:500 for IF	Wako	Cat#019-22291; RRID: AB_664696
Rabbit Anti-NeuN, use 1:500 for IF	Abcam	Cat#ab177487; RRID: AB_2532109
Rabbit Anti-c-Fos (9F6), use 1:500 for IF	Cell signaling technology	Cat#2250; RRID: AB_2247211
Rabbit Anti-Adenylate Cyclase 3, use 1:500 for WB	Thermo Fisher Scientific	Cat#PA5-35382; RRID: AB_2552692
Mouse Anti-beta Actin (clone 7D2C10), use 1:1, 500 for WB	Proteintech	Cat#60009-1-lg; RRID: AB_2687938
Mouse Anti-GAPDH Antibody (clone 1E6D9), use 1:1, 000 for WB	Proteintech	Cat#60004-1-lg; RRID: AB_2107436
Goat Anti-Rabbit IgG (H + L) Highly Cross-Adsorbed Secondary Antibody, Alexa Fluor 594, use 1:500	Thermo Scientific	Cat#A-21206; RRID: AB_2535792
Donkey Anti-Rabbit IgG (H + L) Highly Cross-Adsorbed Secondary Antibody, Alexa Fluor 647, use 1:1, 000	Thermo Scientific	Cat#A-31573; RRID: AB_2536183
Donkey Anti-Goat IgG (H + L) Highly Cross-Adsorbed Secondary Antibody, Alexa Fluor 546, use 1:1, 000	Thermo Scientific	Cat#A-11056; RRID: AB_142628
Anti-Rabbit IgG (H + L) Antibody, DyLight™ 800-Labeled	SeraCare KPL	Cat#5230-0412; RRID: AB_2753123
Anti-Mouse IgG (H + L) Antibody, RbSA, Human Serum Adsorbed, DyLight™ 800-Labeled	SeraCare KPL	Cat#5230-0416
Bacterial and virus strains		
pAAV2/9-pMecp2-spCas9	Hanbio, Shanghai China	N/A
pAAV2/9-U6-AC3 sgRNA-pSyn2-mCherry	Hanbio, Shanghai China	N/A
pAAV2/9-negative control sgRNA	Hanbio, Shanghai China	N/A
pAAV2/9-U6-miR-200b/a sgRNAs-pCMV-GFP	Hanbio, Shanghai China	N/A
pAAV2/9-U6-AC3 shRNA- pCMV-ZsGreen	Hanbio, Shanghai China	N/A
pAAV2/9-U6- negative control shRNA- pCMV-ZsGreen	Hanbio, Shanghai China	N/A
Chemicals, peptides, and recombinant proteins		
$ZnSO_4$	Sigma-Aldrich	Cat#307491
NMDA	Sigma-Aldrich	Cat#M3262
NMLA	Ark Pharm	Cat#4226-18-0
Citral	Sigma-Aldrich	Cat#C83007
Propyl propionate	Sigma-Aldrich	Cat#112267
2- heptanone	Sigma-Aldrich	Cat#537683
Paraformaldehyde	Sigma-Aldrich	Cat#158127
EGTA	Sangon Biotech	Cat#A600077
Sucrose	Sangon Biotech	Cat#A610498
Tissue-Tek O.C.T. Compound	SAKURA	Cat#4583
Triton X-100	Sigma-Aldrich	Cat#T8787
Chemicals, peptides, and recombinant proteins		
DAPI	Sigma	Cat#D9542
Critical commercial assays		
RIPA Lysis and Extraction Buffer	Thermo Fisher Scientific	Cat#89900

(*Continued on next page*)

Continued

REAGENT or RESOURCE	SOURCE	IDENTIFIER
Mir-X™ miRNA First Strand Synthesis Kit	Clontech	Cat#638315
NovaTM SYBR Green PCR Master Green mix	QIAGEN	Cat#208052
Experimental models: Organisms/strains		
Mouse: AC3$^{+/-}$ mice	Storm Lab	N/A
Oligonucleotides		
AC3 guide RNA	GTCCAATTCCAGCCACGGCG	N/A
MiR-200b/a cluster F′ guide RNA	GGAAGTTCCCCGGTCGCAGG *AGG*	N/A
MiR-200b/a cluster R′ guide RNA	GCCTGTCTTCGGCGAATGGT *GGG*	N/A
AC3 siRNA	GCAGATATTGTGGGCTTTA	N/A
Software and algorithms		
ImageJ	NIH	https://imagej.nih.gov/ij/
GraphPad Prism	GraphPad Software Inc	https://www.graphpad.com/scientificsoftware/prism/
Others		
Immobilon-PSQ Transfer Membranes	Merck Millipore	Cat#IPVH00010
Nonfat Dry Milk	Cell Signaling Technology	Cat#9999S
Normal Donkey Serum	Solarbio	Cat#SL050

RESOURCE AVAILABILITY

Lead contact

Further information and requests for resources and reagents should be directed to and will be fulfilled by Zhenshan Wang (zswang@hbu.edu.cn).

Materials availability

This study did not generate new unique reagents.

Data and code availability

This paper does not report original code.

Any additional information required to reanalyze the data reported in this paper is available from the lead contact upon request.

EXPERIMENTAL MODEL AND SUBJECT DETAILS

Experimental animals

All operating procedures and handling methods involving experimental mice were performed in accordance with the "Guiding Opinions on the Treatment of Laboratory Animals" issued by the Ministry of Science and Technology of the People's Republic of China and approved by the Animal Ethics and Care Committee of Hebei University (approval no.: IACUC-2017013). AC3$^{+/+}$ and AC3$^{-/-}$ mice were produced by crossing AC3$^{+/-}$ mice, and the genotypes were determined by PCR. Unless indicated, all the mice used in this study were either 12- to 24-week-old males or one- to 2-day-old newborn pups (not distinguish the sex). All the mice were housed in an SPF animal house (constant temperature of 22–25°C, relative humidity of 40–70%) at the Animal Experiment Center of Hebei University, maintained on a 12-h light/dark cycle and provided food and water *ad libitum*.

METHOD DETAILS

AAV vector packaging

The spCas9 and sgRNA expression plasmids were separately packaged into two AAVs. For the spCas9 AAV, the Mecp2 promoter and spCas9 coding region sequence (CDS) were ligated and cloned into

the AAV2/9 vector to generate AAV-pMecp2-NLS-spCAS9-NLS-spA. For the sgRNA AAV, AC3 sgRNA, miR-200b/a sgRNAs, or NC sgRNA in series with the U6 promoter and ligated with syn2-mCherry or CMV-GFP were cloned into AAV2/9 to generate AAV-U6-AC3/NC sgRNA-pSyn2-mCherry or AAV-U6-miR200b/a/NC sgRNAs-pCMV-GFP. The sgRNA sequences were as follows: AC3 sgRNA (5′-GTCCAATTC CAGCCACGGCG-3′); miR-200b/a F′ sgRNA (5′-GGAAGTTCCCCGGTCGCAGG-3′); and miR-200b/a R′ sgRNA (5′-GCCTGTCTTCGGCGAATGGT-3′).

For the construction of AAV vectors to express shAC3 in the brain, the target sequence 5′-GCAGA TATTGTGGGCTTTA-3′ against mouse AC3 and the U6 promoter sequence were inserted into the AAV-pCMV-ZsGreen vector. AAV packaging was performed by Hanbio (Shanghai, China). The titers of the viral particles were determined by quantitative PCR.

Nasal perfusion of 5% $ZnSO_4$ or AAV

For the 5% $ZnSO_4$-treated mice and 0.9% NaCl-treated mice, WT male C57BL/6N mice aged 3 months were lightly anesthetized with isoflurane, and each nostril was perfused with 20 μL of 5% $ZnSO_4$ ($ZnSO_4$ diluted in saline, Sigma, Cat # 307491) or 20 μL of 0.9% NaCl (control mice).

For MOE-specific AC3-KD, miR-200b/a-KD, and control mice, WT male C57BL/6N mice aged 3 months were lightly anesthetized with isoflurane, and each nostril was perfused with 3 μL of a 1:1 AAV mixture [1.1×10^{12} Vg/mL SpCas9 AAV+ 1.2×10^{12} Vg/mL sgRNA AAV] diluted in 17 μL of saline. Nasal perfusion was performed using a 0.5–10 μL pipette to perfuse the working solution into each nostril.

Stereotactic injection of NMDA/NMLA and AAV

For ablation of the AON and VMH, WT male C57BL/6N mice aged 3 months were lightly anesthetized with isoflurane, and 120 nL of NMDA (Sigma, Cat # M3262, 20 mg/mL PBS) or NMLA (Ark Pharm, Cat # 4226-18-0, 20 mg/mL PBS) was injected into the dorsal AON (AONd; AP: +2.68 mm, ML: ± 1.0 mm, DV: −3.2 mm), lateral AON (AONl; AP: +2.68 mm, ML: ± 1.3 mm, DV: −3.43 mm), and VMH (AP: −1.58 mm, ML: ± 0.5 mm, DV: −5.6 mm) using a stereotaxic injection method. After the operation, the incisions were sutured, and behavioral experiments were started after 4 days of recovery.

For the KD of AC3 expression in the AON and VMH, WT male C57BL/6N mice aged 3 months were lightly anesthetized with isoflurane, and AAV-AC3 shRNA (3.5×10^{12} Vg/mL) or AAV-NC shRNA (3.7×10^{12} Vg/mL) in a volume of 300 nL was injected into the AONd, AONl and VMH nuclei using a stereotaxic approach. Behavioral experiments were performed 4 weeks after injection.

Behavioral assays

Before the behavioral test, the mice were placed in a single cage in the experimental environment for one week for habituation, and the experimenter handled the mice regularly every day to familiarize the mice with the experimenter. The experimenter was unaware of the genotypes of the mice on the day of the experiment. For each assay, the mice were habituated to the testing room for at least 0.5 h, and the behavioral assays were then performed.

Spontaneous locomotor activity test

The spontaneous locomotor activity of the experimental mice was tested by the open field test using the Opto-Varimetrix-3 sensing system (Columbus Instruments). A single mouse was placed in the open field apparatus, and the total distance traveled over a 15-min period was recorded. After each mouse was tested, the open field apparatus was wiped with a cotton ball dipped in 10% alcohol to ensure that residual urine did not affect the next experimental mouse.

Odorant habituation/dishabituation assay

The olfactory detection ability of the mice was tested by the odorant habituation/dishabituation assay. The odorants that were used were male mouse urine (1:50 dilution in water), female mouse urine (1:50 dilution in water), propyl propionate (50 μM), and citral (50 μM), which were prepared in ddH_2O (ready to use). The odorant solutions were dispensed (200 μL each), and ddH_2O was used as a negative control. In the experiment, a cotton swab dipped in ddH_2O was placed in the cage 30 min before the experiment to familiarize the mice with the experimental setup. After habituation to the experimental setup, a cotton swab was

dipped in ddH_2O and placed in the cage, and the number of times the mice sniffed the ddH_2O-containing swab over a 2-min period was recorded. Swabs were then dipped in the other odorants and placed in the cage, and the number of times the mice sniffed the odorants over a 2-min period was recorded. The assay with each odorant and H_2O was repeated twice. A ratio of the number of sniffs the test mice took when the cotton swab with odorant was first introduced to the number of sniffs recorded when the cotton swab with H_2O was first introduced was used for the analysis.

Resident/intruder experiment

The resident/intruder experiment was used to test the male aggression behavior of the experimental mice. The experimental mice were housed individually in cages for approximately 10 days before the start of the experiment, and the mouse cage bedding was not changed for approximately 4 days before the start of the experiment. Ten days later, an unfamiliar WT adult male virgin mouse (defined as the invasive mouse) was placed in the cage of the experimental mouse, at which time the experimental mouse exhibited aggressive behaviors toward the invasive mouse (aggressive behaviors included wrestling/rolling, biting and chasing), and the frequency and duration of the aggressive behavior exhibited by the experimental mouse toward the invasive mouse were recorded over a 15-min period.

Male mating behavior test

After the male aggression experiment, the experimental mice were housed alone for another two days, and during this period, the mice were given sufficient water and food. Unfamiliar WT adult female mice were placed in the resident mouse cages, and the male mating behavior of the experimental mice was monitored over a 15-min period. The frequency and duration of mating were recorded.

Infanticidal behavior test

The infanticidal behavior test was started after the mice were housed alone for 2 days. The mice were removed from their cages, and three 1- to 2-day-old pups were placed in three different corners of the cage. The mice were then placed in the cage with their backs to the pups, the time to approach the pups was recorded, and the time that elapsed before the experimental mice started to commit infanticide was recorded as the infanticide latency period. When the males attacked the pups, the pups were immediately rescued, and the experiments were stopped. The duration of the test was 5 min. If no infanticidal behavior was observed during the 5-min period, the male mouse was defined as a noninfanticidal mouse.

Urine preference assay

Urine was collected from male and female mice of the same genotype. The male and female urine (10 μL) was dropped onto two pieces of filter paper, respectively, and then the two pieces were placed on the opposite sides of the test cage. The test mice were then placed in the cage and allowed a free choice between male and female urine. The investigation time of the male and female urine by the test mice was recorded over a 5-min period.

RNA isolation and qPCR analyses

Total RNA was extracted using the TRIzol method, and first-strand cDNA was synthesized using a Mir-X miRNA First-Strand Synthesis Kit (Clontech, Cat # 638315). The expression of miRNAs was assessed with Nova^{TM} SYBR PCR Master Green mix (Qiagen; Cat # 208052), and the analysis was performed using the $2^{-\Delta\Delta Ct}$ method. All qPCR data were normalized to the expression of U6 (n = 4 mice per group).

Tissue processing and IF

To obtain frozen MOE sections, the mice were anesthetized with isoflurane and perfused with 4% paraformaldehyde (PFA in PBS, pH 7.4). Subsequently, the MOE was dissected, fixed in 4% PFA for 2 days and then decalcified for at least 1 week in 10% EGTA (in PBS). The decalcified MOE tissue was dehydrated in 30% sucrose for 3 days. The dehydrated MOE tissues were embedded in optimal cutting temperature (OCT) medium (Sakura) and cryosectioned at a thickness of 10 μm.

To obtain frozen brain sections, the brains of mice were removed after perfusion with 4% PFA. The brain tissue was fixed in 4% PFA solution for 12–16 h at 4°C and then placed in 30% sucrose for two days until it was completely dehydrated. The brain tissue was subsequently embedded in OCT medium and cut into 40 μm-thick sections using a cryostat (Leica).

For IF, MOE or brain tissue sections were fixed with 4% PFA for 20 min, permeabilized with 0.5% Triton X-100 (with PBS) for 30 min, blocked with 5% donkey serum (0.05 M glycine, 5% donkey serum, 5% BSA, and 0.2% Triton X-100) for 3 h at room temperature (RT) and then incubated with primary antibody solution at 4°C for 16 h. The following primary antibodies were used: OMP (1:500; Wako; Cat # 019-22291), AC3 (1:1,000; Novus; Cat # NBP1-92683), Tuj1 (1:500; Abcam; Cat # ab18207), and NeuN (1:500; Abcam; Cat# ab177487). After incubation with the primary antibody, the sections were subjected to three to four 15-min washes with PBS. The sections were then incubated with secondary antibodies (Alexa 546- or 647-conjugated; 1:1000; Thermo Scientific) for 1–2 h at RT and stained with DAPI (Sigma; Cat # D9542) for 20 min away from light and washed with PBS after each step. The slices were sealed with an anti-quenching sealing agent and observed under an Olympus FLUOVIEW FV3000 confocal microscope. All IF images were acquired under the same conditions and processed identically. ImageJ software and FV10-ASW 4.2 Viewer (Olympus) software was used to process the images.

C-Fos IF

For c-Fos expression analysis, the mice were housed in a single cage for 2 days before the test to return their c-Fos to the baseline level. An equal volume of 2-heptanone (0.1 mg/mL), female urine, or water was evenly spread on the nose of the male test mice. The mice were sacrificed 2 h later for c-Fos IF analysis.

The sections were preincubated for 2 h in 10% goat serum (10% goat serum, 3% BSA, and 0.25% Triton X-100) at RT and then incubated for 48 h with an anti-c-Fos antibody (1:500; Cell Signaling Technology; Cat # 2250) at 4°C. The sections were then incubated with secondary antibodies (Alexa 594-conjugated; 1:500; Thermo Scientific) for 2 h at RT and stained with DAPI. Washes with 1x PBS/0.1% Triton X-100 (PBST) were performed after each step. The slices were observed under an Olympus BX53 fluorescence microscope. To determine the number of c-Fos-positive cells throughout the mitral and granular cell layers of the AOB and MOB, 3 sections were selected from each mouse for averaging.

WB analysis

Total protein (from MOE, AON, and hypothalamic tissues) was extracted using RIPA lysis buffer, and the concentration was measured by the BCA method. Equal amounts of protein were separated by sodium dodecyl sulfate–polyacrylamide gel electrophoresis (SDS–PAGE) and transferred to polyvinylidene difluoride (PVDF) membranes (Millipore). The PVDF membranes were blocked at RT for 2 h (5% nonfat dry milk in TBS), incubated with AC3 primary antibody (1:500; Invitrogen; Cat # PA5-35382) at 4°C for more than 24 h, subjected to four 5-min washes with PBST, incubated with secondary antibody (conjugated to 680- or 800-nm fluorophores, SeraCare KPL, 1:10,000 in TBST buffer) for 2 h at RT, imaged with Odyssey software (Li-Cor). The grayscale value of the target protein was quantified using Odyssey software (Li-Cor), and the relative expression level of the protein was calculated as the grayscale value of the target protein relative to the grayscale value of the control protein. Actin or GAPDH was used as a loading control.

QUANTIFICATION AND STATISTICAL ANALYSIS

Statistical analysis

The statistical analysis was conducted with GraphPad Prism 7 software. Student's t test was used to analyze differences between two treatment groups. The data are shown as the means ± standard errors of the mean (SEMs). *$p < 0.05$, **$p < 0.01$, ***$p < 0.001$, and ****$p < 0.0001$ were considered to indicate statistical significance. Statistical information for each experiment can be found in the figures and corresponding figure legend.